Liquid Crystals
Publication details, including instructions for authors and subscription information:
http://www.informaworld.com/smpp/title~content=t713926090

Molecular complexity and the control of self-organising processes

John W. Goodby[a]; Isabel M. Saez[a]; Stephen J. Cowling[a]; Julita S. Gasowska[a]; Robert A. MacDonald[a]; Susan Sia[a]; Paul Watson[a]; Kenneth J. Toyne[b]; Michael Hird[b]; Robert A. Lewis[b]; Seung-Eun Lee[c]; Valerij Vaschenko[d]
[a] The Department of Chemistry, The University of York, York, UK [b] Department of Chemistry, The University of Hull, Hull, UK [c] R&D Technical Centre, Merck Advanced Technologies Ltd, South Korea [d] STC 'Institute for Single Crystals', NAS of Ukraine, Kharkov, Ukraine

To cite this Article Goodby, John W. , Saez, Isabel M. , Cowling, Stephen J. , Gasowska, Julita S. , MacDonald, Robert A. , Sia, Susan , Watson, Paul , Toyne, Kenneth J. , Hird, Michael , Lewis, Robert A. , Lee, Seung-Eun and Vaschenko, Valerij(2009) 'Molecular complexity and the control of self-organising processes', Liquid Crystals, 36: 6, 567 — 605
To link to this Article: DOI: 10.1080/02678290903146060
URL: http://dx.doi.org/10.1080/02678290903146060

Liquid Crystals,
Vol. 36, Nos. 6–7, June–July 2009, 567–605

Taylor & Francis
Taylor & Francis Group

INVITED ARTICLE

Molecular complexity and the control of self-organising processes

John W. Goodby[a]*, Isabel M. Saez[a], Stephen J. Cowling[a], Julita S. Gasowska[a], Robert A. MacDonald[a], Susan Sia[a], Paul Watson[a], Kenneth J. Toyne[b], Michael Hird[b], Robert A. Lewis[b], Seung-Eun Lee[c] and Valerij Vaschenko[d]

[a]*The Department of Chemistry, The University of York, York YO10 5DD, UK;* [b]*Department of Chemistry, The University of Hull, Hull HU6 7RX, UK;* [c]*R&D Technical Centre, Merck Advanced Technologies Ltd, South Korea;* [d]*STC 'Institute for Single Crystals', NAS of Ukraine, 61001 Lenina Avenue 60, Kharkov, Ukraine*

(Received 2 June 2009; final form 16 June 2009)

In this article we investigate the complexity of the molecular architectures of liquid crystals based on rod-like mesogens. Starting from simple monomeric systems founded on fluoroterphenyls, we first examine the effects of aromatic core structure on mesophase formation from the viewpoint of allowable polar interactions, and then we model these interactions as a function of terminal aliphatic chain length. By incorporating a functional group at the end of one, or both, of the aliphatic chains we study the effects caused by intermolecular interfacial interactions in lamellar phases, and in particular the formation of synclinic or anticlinic modifications. We then develop these ideas with respect to dimers, trimers, tetramers, etc. We show, for dendritic systems, that at a certain level of molecular complexity the local mesogenic interactions become irrelevant, and it is gross molecular shape that determines mesophase stability. The outcome of these studies is to link the complexity of the molecular interactions at the nanoscale level, which lead to the creation of the various liquid-crystalline polymorphs, with the formation of mesophases that are dependent on complex shape dependencies for mesoscopic supermolecular architectures.

Keywords: liquid crystal polymorphs; liquid crystal modelling; ferroelectric and antiferroelectric liquid crystals; dimers; trimers and tetramers; polymer liquid crystals; dendrimers; supermolecular liquid crystals

1. Introduction

Up until the last decade, the basic design of the molecular structures of thermotropic liquid crystals had changed very little. Materials that exhibit liquid crystal mesophases typically have molecular structures that can be classed as spherical, rod-like or disc-like, with combinations of the two producing phasmidic liquid crystals. The discovery that materials with bent molecular structures exhibited whole new families of mesophases has led the charge towards investigating the liquid crystal properties of materials with widely varying molecular topologies: from pyramids to crosses to dendrites. For materials with rod-like molecular shapes the prototypical molecular design involves the incorporation of a central aromatic, heterocyclic or alicyclic core unit, to which are attached terminal aliphatic chains (*1–3*), thereby engendering dichotomous structures with rigid or semi-rigid sections surrounded, or segregated, by flexible fatty chains, see structures **1** and **2** in Figure 1. When molecules with this type of architecture self-organise, they generally do so with their rigid, aromatic parts tending to pack together and their flexible/dynamic aliphatic chains orienting together. Thereby the overall system becomes so-called '*locally microphase segregated*'. Consequently, the main target of material design has been, by default, the variation in the structure of the central core region of the molecules in the belief that the core is more important in influencing mesophase incidence, mesophase temperature range, isotropisation point, melting point, mesophase sequence, dielectric and optical anisotropy, elastic coefficients and the reorientational viscosity associated with the mesophase (*4–8*).

One of the more important applications of liquid crystals is in display devices. The bedrock of the liquid crystal display (LCD) industry has been built on the twisted nematic liquid crystal display (TNLCD) device, which was developed in the early 1970s. Nematic liquid crystals designed for applications in TNLCD technologies typically have strongly polar groups situated at one terminus of the molecular structure to engender large positive dielectric anisotropies (*9–13*). The structural design for nematogens with such anisotropies are exemplified by the cyanobiphenyls shown in structure **3** in Figure 1. Similarly, modern LCD TVs utilising in-plane switching (IPS) modes (*14–16*) with wide viewing angles also employ nematogens with positive dielectric anisotropies. Conversely, competitive LCD TV technologies based on vertically

*Corresponding author. Email: jwg500@york.ac.uk

ISSN 0267-8292 print/ISSN 1366-5855 online

DOI: 10.1080/02678290903146060
http://www.informaworld.com

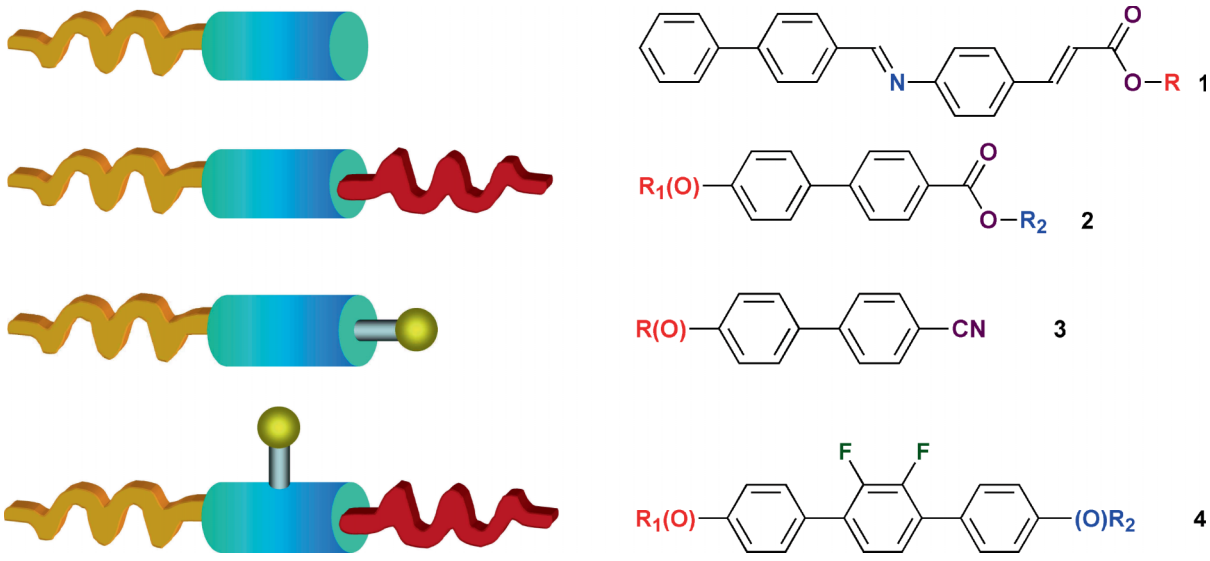

Figure 1. Typical material design for rod-like liquid crystals (*9*, *20*, *27*, *28*). Materials **3** and **4** show the design of liquid crystals found in display devices.

aligned nematics (VAN) modes utilise materials with negative dielectric anisotropies (*15–19*). Such materials are designed to have polar groups situated in a lateral position relative to the long axes of the molecules as exemplified by the difluoroterphenyls, **4**, shown in Figure 1 (see also (*20*)). In addition to the design and development of materials for applications in VAN LCDs, materials such as **4**, with negative dielectric anisotropies, are of practical use in smectic devices, for example those based on the surface-stabilised ferroelectric liquid crystal display (SSFLCD) geometries (*21*) or $\tau V_{\min}$ ferroelectric displays based on dielectric biaxiality (*22–24*). Ferroelectric devices offer fast response times and bistable operation, and are of practical use in the eyepieces of digital cameras (*25*, *26*). Owing to the relevance of fluoro-substituted terphenyls to both nematic and smectic displays, we use this moiety as the primary, prototypical central core structure in the systematic comparisons made in this concept article.

If we consider the common 'materials design' comprising a central core unit with two attached peripheral groups, usually aliphatic chains, as depicted by structures **2** and **4** in Figure 1 (see (*9*, *20*, *27*, *28*)), then it is easy to understand how the differences in interactions between the aliphatic flexible chains and the aromatic rigid cores can lead to so-called '*microphase segregation*' where the similar parts of the molecules pack together and repel the dissimilar parts. However, the design of the molecular construction can be comprehended at a deeper level. If the construction is thought to be made up of three units, one being the aromatic core and the other two by different flexible chains, then for a simple design there are eight possible arrangements of the sub-units depending on their orientation of attachment, as shown in Figure 2. Thus, the complexity of a simple molecular architectural design is increased eightfold, which is reflected in the melting behaviours, mesophase sequences, transition temperatures and physical properties of the mesogens so-created. As a consequence the development of property–structure correlations has involved the synthesis of many families of materials where the central core has been kept constant and the peripheral flexible units have been varied (usually in length), or the flexible units have been arranged to be constant and the central core has been varied (*1*).

2. Complexity associated with the central core

2.1 Mono-substitution in the core

The first approach we take into the investigation of intermolecular interactions in mesomorphic systems is where the peripheral flexible units are maintained/retained, but the central rigid core is varied. When we examine the complexity associated with the design of chemical structure, we find that the simple issue associated with the position of fluoro-substitution in a given core unit can have very marked effects on transition temperatures, melting and clearing points, and mesophase formation. Fluorine substitution does not particularly change the overall shape of the core as a fluoro-substituent is not very different in size to the hydrogen it replaces, however, the fluoro-substituent imparts polarity to the system, so this study involves

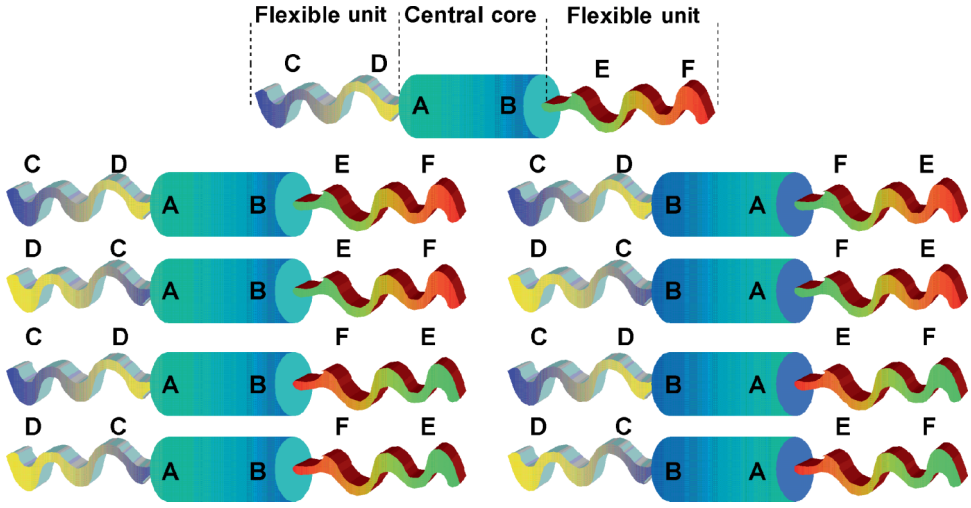

Figure 2. Possible constructions for a simple mesogen possessing a rigid aromatic core and two different peripheral flexible chains.

little change to the molecular shape, but large changes to polarity and location of dipole moments.

Thus, consider the family of materials shown in Figure 3 (*20*, *29–33*). The terminal chains are the same in each material and all of the materials are *para*-terphenyls. Without any fluoro-substituents the '*low polarity*' parent material exhibits smectic A and B phases where the molecules are arranged in layers with their long axes on average perpendicular to the layer planes. The incorporation of one fluoro-substituent in the central aromatic ring results in the addition of G, smectic C and nematic phases with the melting point falling in comparison by 135°C. Moreover, unlike the parent material, most of these phases possess structures where the molecules are tilted with respect to the layer planes. For the three mono-fluoroterphenyl isomers shown in Figure 3, it can also be seen that the phase sequences vary greatly

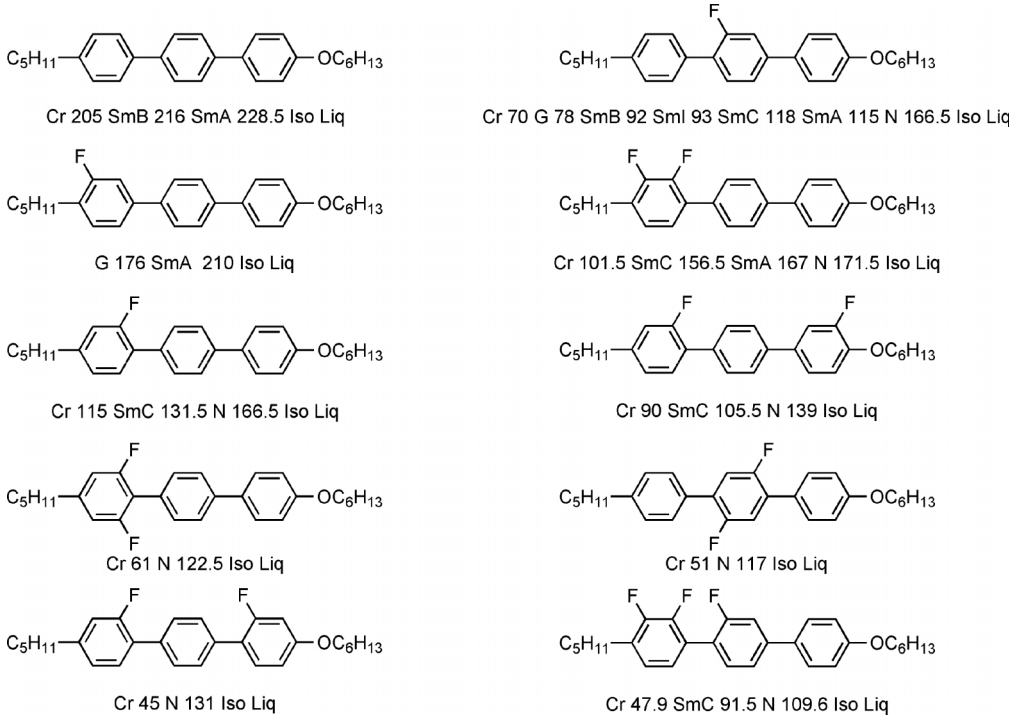

Figure 3. Mesophase type and transition temperatures (°C) as a function of fluoro-substitution in 4″-hexyloxy-4-pentylterphenyls (*20*, *29–33*).

with the location of the site of substitution. This figure also shows that as the fluoro-substituents increase in number there is a greater tendency for the materials to exhibit nematic phases, i.e. disordering increases with increasing polar substitution. Melting points are often found to fall with increasing degree and the location of fluoro-substitution. Thus, the unsubstituted terphenyl has the highest melting point and is of no practical use in electrooptic devices, whereas the fluoro-substituted materials, which exhibit nematic and/or smectic C phases are of particular interest in VAN LCDs and SSFLCDs, respectively.

Apart from these general observations, the literature materials in Figure 3 (*20*, *29–33*) show no systematic pattern of melting behaviour. This is possibly due to the fact that the full set of isomers is not available, however, some smaller subsets have been reported (*31*). For example, information on the monofluoro-substituted terphenyls is available. For the monofluoro-substituted 4″-hexyloxy-4-pentylterphenyls there are six possible isomers which can potentially increase the complexity of the system, as shown in Figure 4. Where the fluoro-substituent is located in an inner position nematic phases are favoured, but when the substituent is located in the terminal rings pointing away from the core (outer), no nematic phases are observed and smectic phases predominate. This is similar to results obtained for the parent system which also does not exhibit a nematic phase. Interestingly, when the fluoro-substituent is located at the centre ring tilted hexatic phases, in the form of the smectic I phase (*34*), are found. The structural changes observed on cooling from the isotropic liquid are shown in the diagram in Figure 5 for a material with a central fluoro-substituent.

Although the results obtained for the phase sequences and accompanying transition temperatures might seem at first glance to be uncorrelated, it is possible to group the isomers into three sets as shown in Figure 4. The outer position for fluoro-substitution favours orthogonal mesophases; substitution at the central ring favours hexatic phase structuring; and, finally, inner substitution in the outer rings favours the formation of tilted mesophases. If it is presumed for the terphenyls that the core dominates mesophase formation, then it is the nature of the interactions and the packing of the terphenyl cores together that determines mesophase structure (orthogonality and tilt) and hence stability. The steric shape and average conformational structure, together with the associated molecular dynamics, consequently affect the packing of the core units together. Conversely, it is the dipolar and quadrupolar couplings that determine the most stable packing arrangements of the terphenyl cores. Thus, the steric bulk allows for certain polar interactions to be

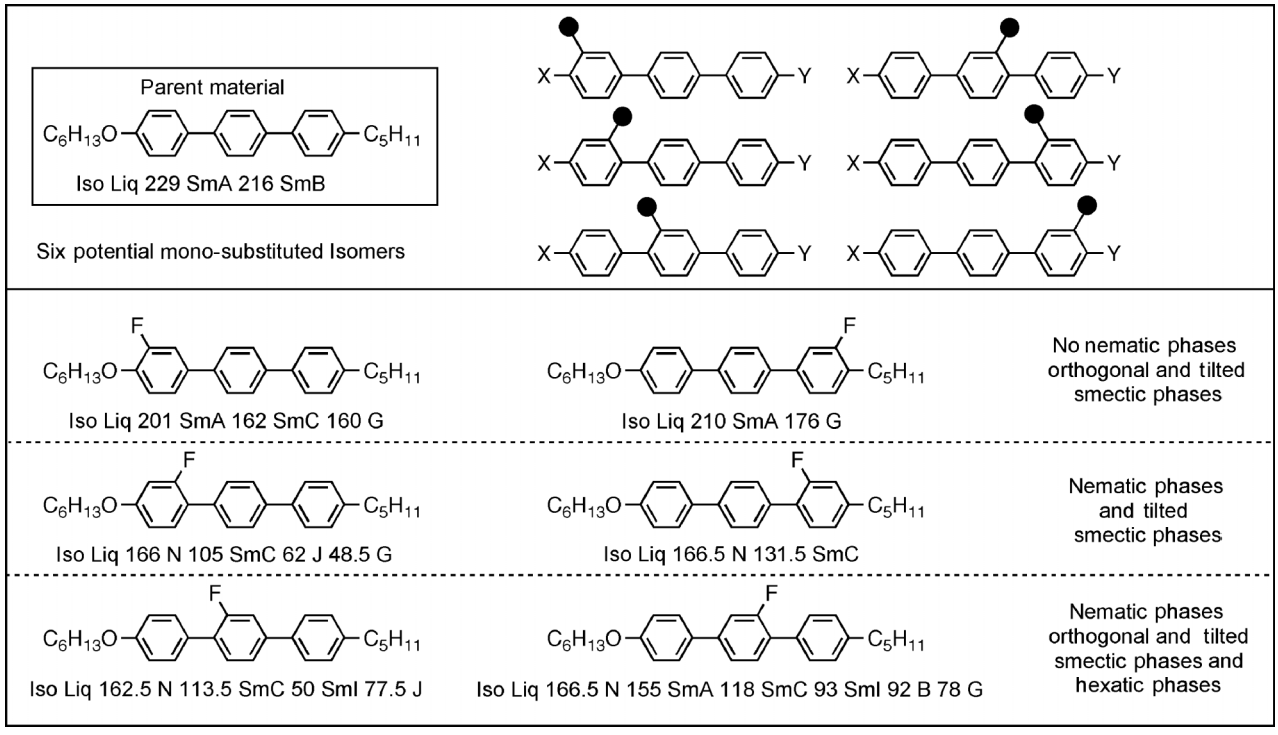

Figure 4. Possible isomers, and the effect of position of substitution on transition temperatures (°C) for the monofluoro-substituted terphenyls.

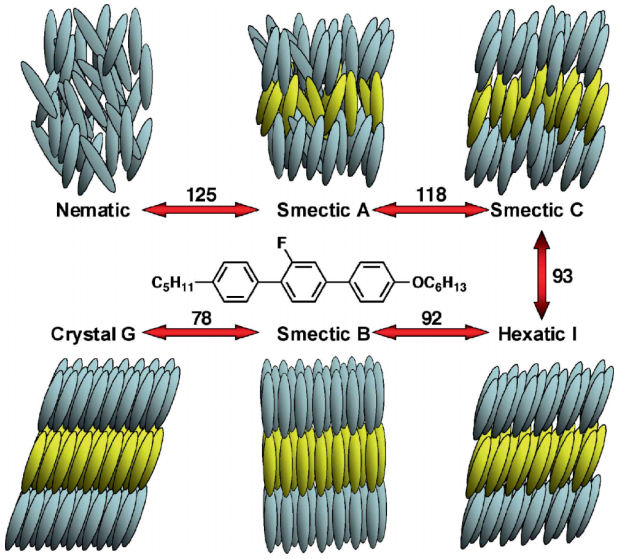

Figure 5. The change in the structures of the liquid crystal phases formed when the laterally fluoro-substituted terphenyl is cooled from the isotropic liquid or heated from the anisotropic plastic crystal G phase.

favoured over others as a function of intermolecular separation.

Ideally, modelling of the system would involve the passing of one molecule across the surface of another and measuring the strength of the dipolar and quadrupolar couplings as a function of the intermolecular separation, which itself will vary as a function of the degree of overlap of the terphenyl cores. Each stable orientation will have an associated *Lennard–Jones* potential energy well. The orientations with the lowest energy levels might then be expected to provide the basic molecular orientations, and hence building blocks for mesophase formation and stability. In particular, the most stable orientations will determine whether a material will exhibit a tilted or orthogonal lamellar phase. In the early investigations of smectic C phases, a number of theories were developed to explain why the molecules tilt at the smectic A to smectic C transition, but none were found to adequately describe and predict this process. However, our proposed model steers a neat course between the 'out-board lateral dipolar' model introduced by McMillan (*35*), and the 'stacking of chairs' steric model of Wulf (*36*) for smectic C phase formation, and moreover its simplicity makes it comprehensible in comparison to other theories (*37*). In addition, the concept is able to explain phase changes other than the smectic A to smectic C transition, for example the B to E phase transition (*38*).

Furthermore, the model can be used to investigate the packing arrangements for the monofluoro-substituted terphenyls shown in Figure 4. In order to investigate the packing arrangements of the core units, the monofluoro-substituted 4″-methoxy-4-methylterphenyl can be used as representative examples of the terphenyl core system. It can be seen from these studies that the packing arrangements of two antiparallel core units for each isomer (for the director of the phase, $n = -n$) can be stabilised through quadrupolar interactions, the lowest energy and most stable orientations for which are shown in Figure 6. In some cases, direct overlap of the core units is favoured (e.g. Figure 6(c) and (d)), which would result in orthogonal phases being formed, whereas for the other cases the cores are staggered favouring tilted phases (e.g. Figure 6(a) and (e)). The lateral interaction for Figure 6(c) and (d) would also be relatively strong, resulting in smectic phases being preferred over nematic phases, conversely the intermolecular repulsions for the other arrangements are probably strong enough to prevent the formation of lamellar phases and hence nematic phases persist. Arrangements depicted in Figure 6(b) and (e) are also interesting because the overlap is much less pronounced for Figure 6(e) than Figure 6(b); this is because the fluoro-substituent is further away from the methoxy group in Figure 6(b) than Figure 6(e). This results in better overlap of the core units and orthogonal phases such as smectics A and B being more stable in the case of the equivalent monofluoro-substituted 4″-methoxy-4-methylterphenyls. However, in both cases hexatic phases also become stabilised, suggesting that there are reasonably strong lateral repulsive forces present.

2.2 *Multiple substitution in the core*

If the number of substituents in the terphenyl core is increased from one to two, then the possible structural isomers increases from 6 to 24, as shown in Figure 7. This increases the complexity fourfold, which is beneficial for the development of multicomponent mixtures for applications in display and photonic devices. Of the 24 isomers, half have their substituents in locations where their positions/orientations are fixed and cannot be varied via molecular dynamics to give a variety of conformers (the top 12 structures in Figure 7), whereas the other 12 can have conformational variations created through inter-annular bond rotation (bottom 12). Thus, the latter 12 have a higher degree of complexity than the first 12 isomers. Typically, it is the first 12 that have fixed positional relationships between the substituents that are of more practical use in VAN and SSFLCD displays.

For some of the first 12 isomers, the two substituents occupy the 2 and 3 positions on one side of the aromatic rings. In this arrangement, the two substituents can act as one. If the substituents are methyl, together the two create a large bulky lateral group,

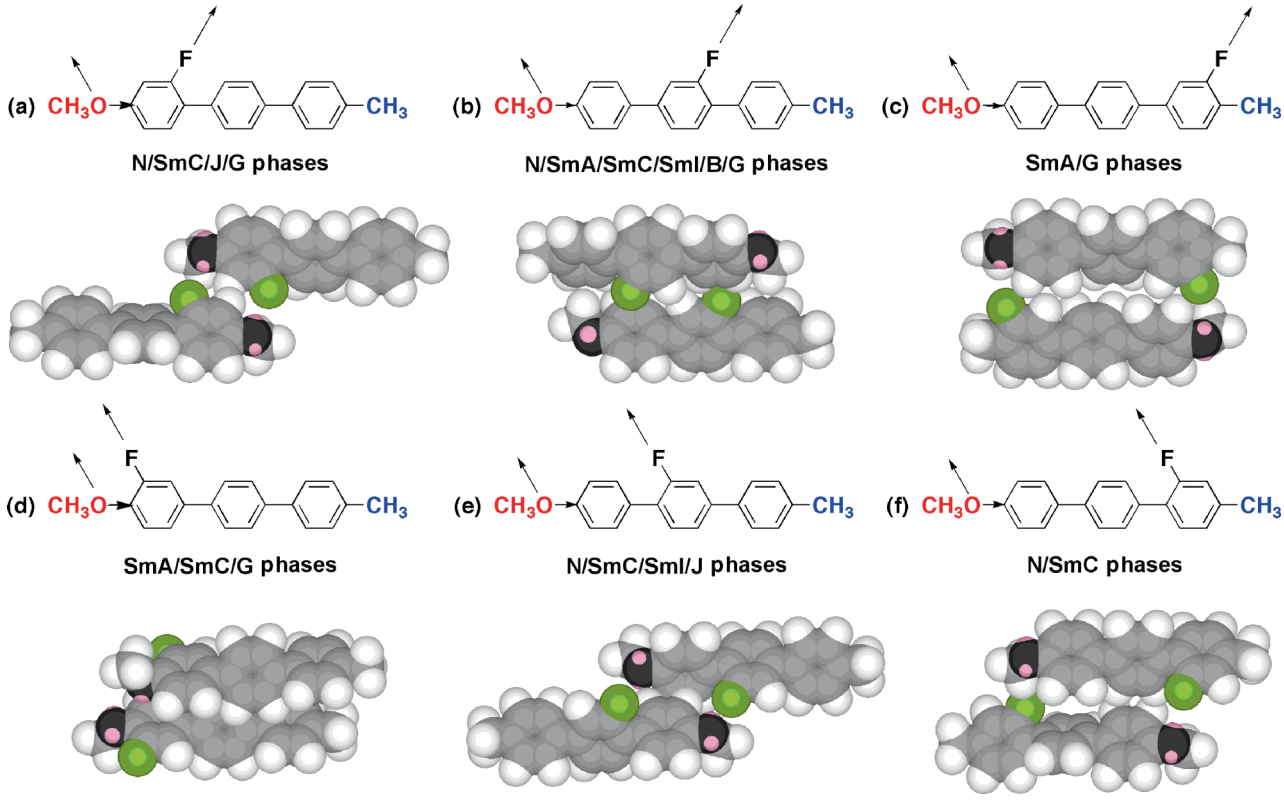

Figure 6. The six isomers of monofluoro-substituted 4″-methoxy-4-methylterphenyl showing the mesophases exhibited for the equivalent monofluoro-substituted 4″-hexyloxy-4-pentylterphenyls. Minimised structures of the isomers were determined in the gas phase. The models are depicted using ChemDraw 3D™.

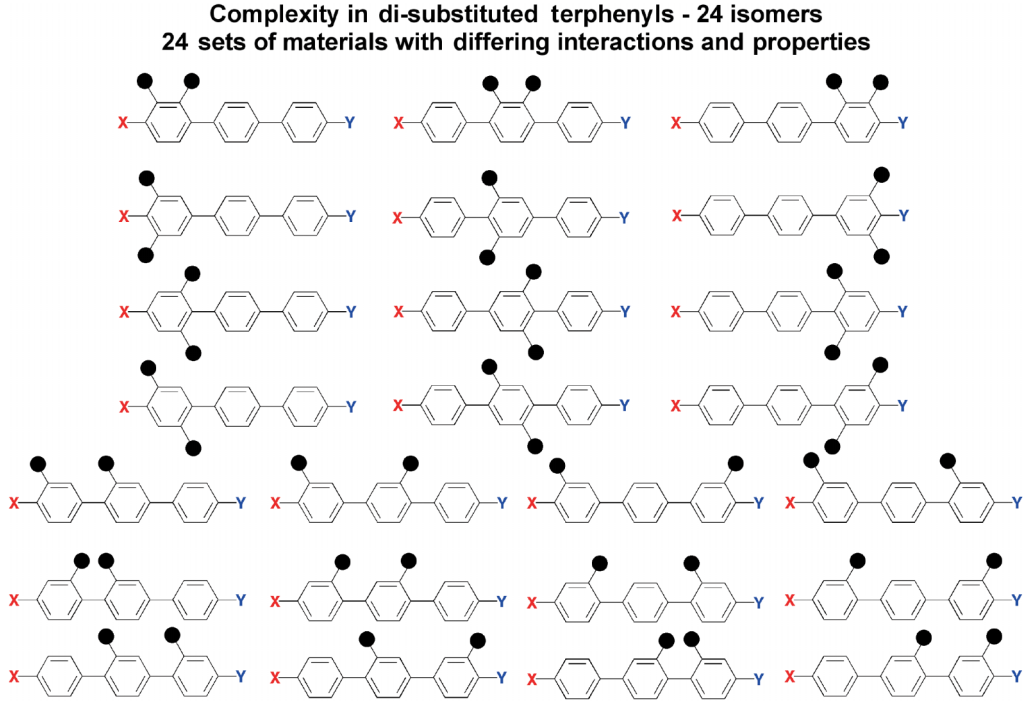

Figure 7. The twenty-four isomers of the di-substituted 4″-alkoxy-4-alkylterphenyls.

but for two lateral fluoro-substituents, acting together they generate a large dipole perpendicular to the long axis of the molecule. Thus, for these isomers the complexity is effectively reduced, and this is mirrored in their phase behaviour, transition temperatures and physical properties. Figure 8 shows a family of three difluoro-4″-octyloxy-4-pentylterphenyls, which all exhibit nematic and smectic C phases, and in addition the two isomers (Figure 8(a) and (c)) with the difluoro-substituents in an outer ring of the terphenyl unit exhibit smectic A phases. Thus, the phase behaviour of the family maps on to that exhibited by the mono-fluoroterphenyls as discussed earlier. The transition temperatures for the two isomers with fluoro-substituents in the outer rings (Figure 8(a) and (c)) are also very similar, however, the dielectric anisotropy of the left-hand isomer (Figure 8(a)) is twice the value of that found for the other isomer (Figure 8(c)). This is because the oxygen associated with the octyloxy chain is conjugated to the fluoro-substituent, hence the combined lateral dipole is larger. The larger dipole at one end of the molecule (Figure 8(a)) has the effect of reducing the transition temperatures by approximately 10°C, whereas the more symmetric isomer in terms of its polarity (Figure 8(c)) has a stronger quadrupolar coupling leading to higher transition temperatures.

The reduced complexity provided by 2,3-di-substitution of the core has been utilised in the development of host smectic C mixtures for applications in ferroelectric liquid crystal devices, in particular those using $\tau V_{\min}$ switching modes. Doping of a host that exhibits a nematic, smectic A, smectic C phase sequence with a structurally matched chiral material can provide a ferroelectric blend that has desirable properties for display applications. Figure 9 shows the constituents of a host mixture marketed by Kingston Chemicals Ltd, which when doped with a chiral difluorobiphenyl, gives a ferroelectric blend that exhibits a very fast response to applied electric fields.

When three substituents are introduced into the terphenyl core, the complexity increases still further, until six substituents are reached whereupon it symmetrically falls again. However, there are possibilities for a reduction in the architectural complexity via interactions between the substituents on adjacent aromatic rings which reduce the number of

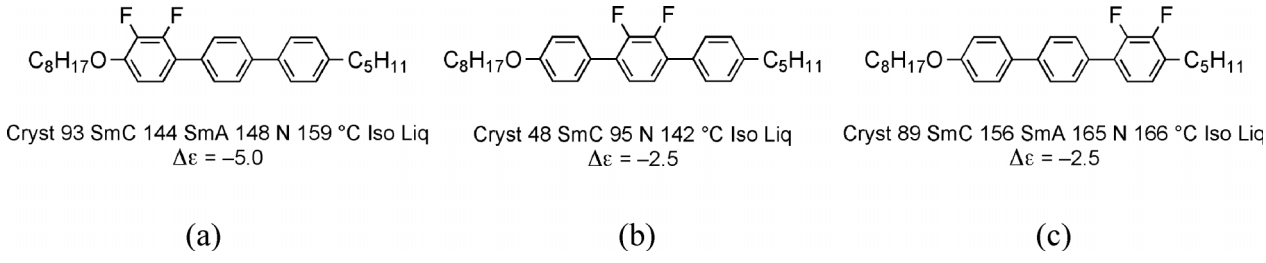

Figure 8. Comparison of transition temperatures (°C) and dielectric anisotropies for a family of difluoro-4″-octyloxy-4-pentylterphenyls.

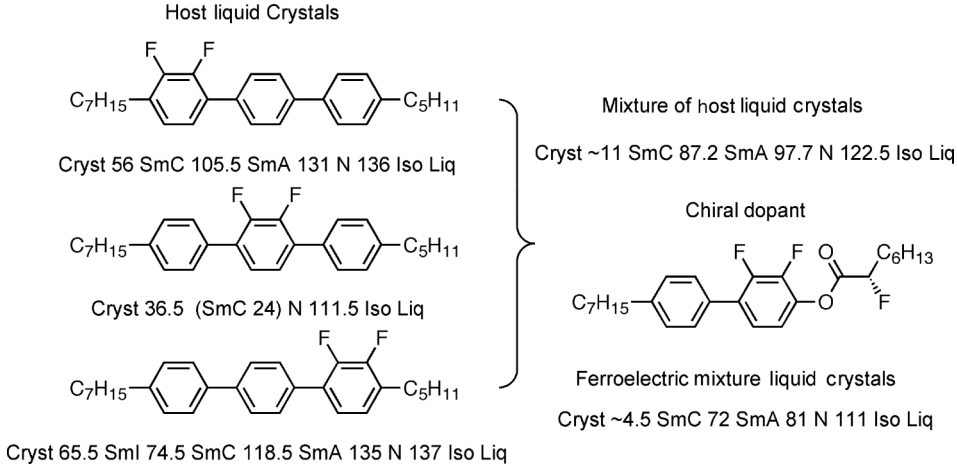

Figure 9. Host smectic C mixture marketed by Kingston Chemicals Ltd for doping with a chiral material to produce a ferroelectric blend that responds quickly to applied electric fields.

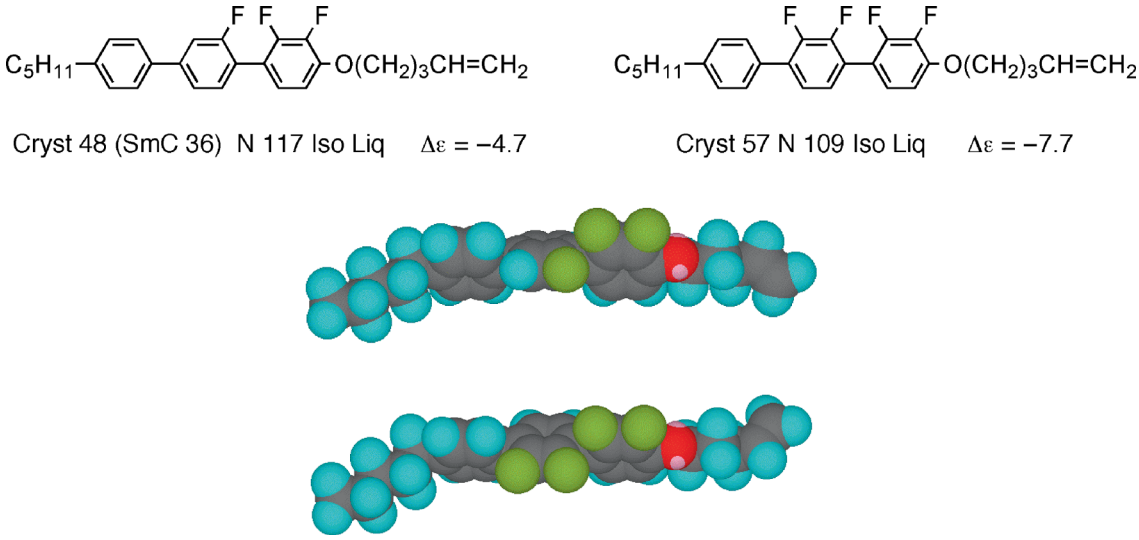

Figure 10. Comparison of dielectric anisotropies of tri- and tetra-fluoro-substituted terphenyls (top), and their minimised structures in the gas phase (bottom). The models are depicted using ChemDraw 3D^{TM}.

conformations. For example, compare the dielectric anisotropies determined for the trifluoro- and tetrafluoro-substituted terphenyls shown in Figure 10 (top) (see also (*39*)). The materials exhibit nematic phases and have similar clearing points, however, the tetrafluoro-substituted material has a negative dielectric anisotropy that is over 60% larger than the value of the trifluoro-substituted material.

The larger negative dielectric anisotropy for the tetrafluoro-substituted compound can be rationalised as follows. The inter-annular twisting about the 1-1′-carbon-carbon bond of the terphenyl core unit suggests that the dipole associated with fluoro-substituents (one or two) located on the centre ring can oppose the dipole associated with the adjacent outer ring that carries two fluoro-substituents, thereby minimising the overall lateral dipole. As a consequence, the opposed dipoles would reduce the negative value of the perpendicular permittivity. The fact that the perpendicular permittivity has a larger negative value for the tetrafluoro-substituted terphenyl indicates that dipolar effects of the fluoro-substituents are additive rather than subtractive. Modelling of each compound, in the gas phase using energy minimisation techniques, suggests that the fluoro-substituents lie on the same side of the molecule, see Figure 10 (bottom). Thus, there appears to be through-space coupling between the fluoro-substituents located on adjacent rings, which may be reinforced in electrical field experiments, even though the molecules are in dynamic motion about their long axes in the liquid crystal state.

The coupling through an inter-annular twist in an 'atropisomeric-like' effect means that the trifluoro- and tetrafluoro-substituted systems are acting as though the three or four fluoro-substituents are enlarged single polar entities, and thus the complexity is relatively reduced.

So far the discussion has focused on systems where multiple substituents have the same chemical identity. However, it is also possible to have substituents with different identities. For example, Figure 11 shows three examples of terphenyls where the core has two substituents with different identities (*40*). Although three examples have been reported, six isomers are required in order to begin developing property–structure correlations. The remaining three have either not been prepared or are not reported in the literature. Even though there appears to be a trend of increasing orthogonal lamellar phase stability from left to right across the three materials in the figure, it is not

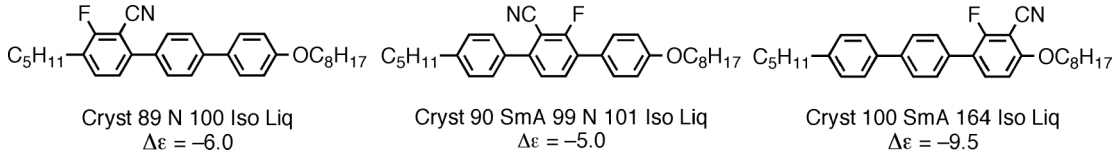

Figure 11. Terphenyls with two substituents of differing chemical identities.

possible to make this conclusion with certainty without knowing the phase behaviour of the other three isomers.

3. Complexity in the peripheral tails

The central cores tend to give the packing of the molecules in calamitic mesophases rigidity with respect to the mesophase structure, whereas the peripheral tails provide softness and properties of 'microphase segregation'. Nevertheless, the dimensionality of the tails can affect mesophase formation and polymorphism particularly in layered smectic phases. In order to appreciate their full effectiveness in mesophase formation and stability, it is best first to construct dynamic models of the molecules in their mesophase environment. This first involves modelling of the motion of the molecules about their long axes: this gives an appreciation of the rotational volumes occupied by the molecules. The second part is to examine how the molecules pack together in parallel and antiparallel arrangements, and finally to map onto those packing organisations the dipolar and quadrupolar interactions. In this section, the n-alkyl 4′-n-alkoxybiphenyl-4-carboxlates (nmOBCs) (*28*, *41*) will be used as the examples because a considerable amount of data is available on their transition temperatures and mesophase structures, e.g. 65OBC and 45OBC were the first materials to be shown to exhibit hexatic phases (*42*, *43*).

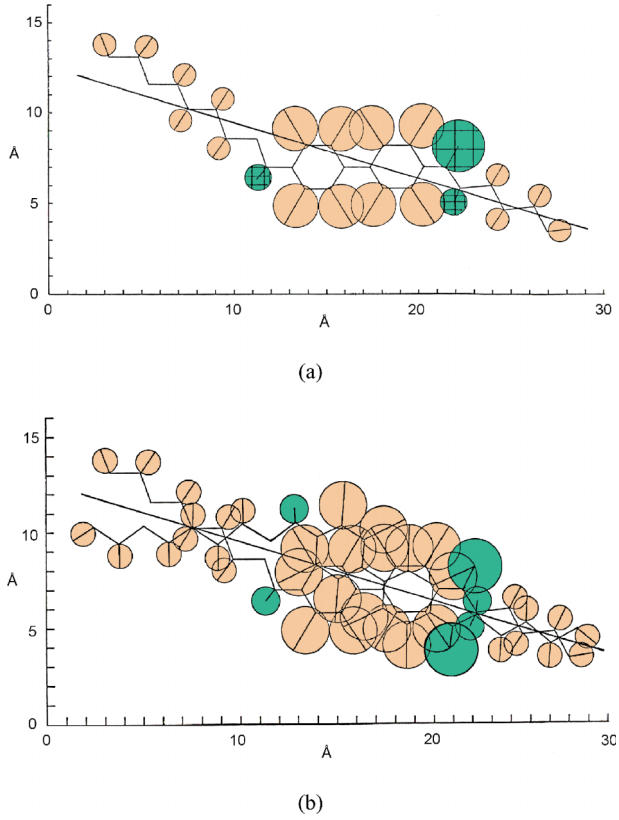

Figure 12. (a) Determination of the minimum inertia axis for butyl 4′-n-octyloxybiphenyl-4-carboxylate (48OBC); (b) cross-sectional area of the material as it rotates about its long axis.

3.1 Determination of the molecular rotational cross-sectional area

In its simplest form the calculation of the shape of a molecule as it rotates about its long axis can be made by projecting the molecular structure of the mesogen onto a flat surface (*38*). Typically, this involves drawing out the molecular structure in its all-*trans* conformation (other conformations can be used if required) by use of known bond lengths and bond angles; this requires that bonds sticking out of the plane must be projected back into it as though the molecule were flat. This provides the simple 'σ' bond framework of the '*molecular skeleton*'. The molecule can then be given its '*body*' by the addition of *van der Waals* radii associated with the electrons of each atomic centre, as shown in Figure 12(a) for butyl 4′-n-octyloxybiphenyl-4-carboxylate (48OBC). The flat molecular projection can now be placed on Cartesian axes of arbitrary location. The positions of all of the atomic centres can be related directly to these axes, and the position of the long axis can now be made via determining the minimum mass inertia axis through the atomic centres. Once the equation of the line has been determined it can be drawn on the graphical description of the mesogen, see Figure 12(a). This line depicts the molecular long axis of the molecule in a desired conformational structure, which is all *trans* in this case.

If the molecule is allowed to rotate about this long axis then a representation of the volume ascribed in space by this motion can be derived by using the axis as a plane of reflection. Thus, by reflecting mass centres across this line it is possible to project the shape of the molecule rotated through an angle of 180° about the long axis on top of the original molecular projection, as shown in Figure 12(b). This composite shape then represents the cross-sectional area of the volume of space occupied by the molecule as it rotates about its long axis. Thus, the swept out volume of rotation has a radius of rotation that is a minimum (that is, if the rotational volume of the molecule is contained within a cylinder, so that the molecule just touches the sides of the cylinder, then the diameter of the cylinder will be a minimum). When such cylinders are closely packed together in layers side by side the effective volume occupied by the molecules, with complete freedom of rotation, will also be a minimum.

3.2 Packing of mesogens together

Having determined the shape of the cross-sectional area of the molecule as it rotates about a known long axis, the shape can be used to investigate the packing requirements of the mesogen under consideration. For example, if two cross-sectional shapes are taken together they can be arranged to pack together in parallel (see Figure 13(a)) or antiparallel orientations (see Figure 13(b) and (c)). In the parallel orientation the nearest dipolar interactions occur through the ester and ether oxygens, depicted by the (green) circles in the figure. Although the molecules have polarisable core regions, the lateral dipoles repel in this orientation, and the longitudinal dipoles, shown as (red) arrows, are parallel thereby making it difficult for the structure to be stabilised by the formation of a quadrupole, see Figure 14(a). The antiparallel arrangements, however, have lateral interactions that are constructive, and longitudinal polarisabilities that reinforce, thereby creating a quadrupolar system as shown in Figure 14(b) which stabilises the molecular packing. Thus, the antiparallel arrangements are more stable than the parallel arrangements.

If the antiparallel arrangements are examined more carefully it can be seen that the position where the ends of the molecules are located together, as shown in Figure 13(b), has its polar groups further apart than if the molecules are staggered with respect to one another, as shown in Figure 13(c). This is the most stable orientation, and it induces a tilted arrangement of the mesogens when the peripheral chains are taken into account. The tilt can be estimated from this figure to be approximately 17°, which is close to the determined value.

If the liquid crystal properties of the homologous series of the alkyl 4′-n-octyloxybiphenyl-4-carboxylates (for alkyl equal to methyl to alkyl equal to decyl) are examined, it is found that the early homologues in the series exhibit orthogonal smectic A, hexatic B and crystal E phases, whereas the homologues of intermediary chain length exhibit smectic A and smectic C phases, and the longer chain length homologues just smectic A phases. Thus, as the ester chain length is increased the liquid crystal phases change from being orthogonal with polymorphism leading to phases with organised structures, then to phases being predominantly tilted, and finally to mesophases having disorganised layered structures. The central core structure is constant, and so the change in mesophase type is being driven to some degree by the peripheral chains, and in particular their relative lengths.

Figure 15 (centre) shows the experimental data for the changes in mesophase type as the homologous series is ascended. It can be seen that the hexatic B and crystal E phases fall away sharply once the ester chain length is increased beyond three carbon atoms (*28*, *41*), at which point it becomes more flexible. The tilted smectic phase is injected at the butyl

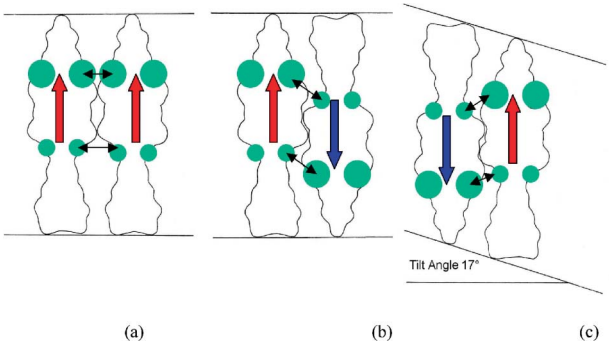

Figure 13. Packing of the shapes of the cross-sectional areas of butyl 4′-n-octyloxybiphenyl-4-carboxylate. (a) Parallel, (b) antiparallel with the ends of the molecules located together, and (c) a staggered antiparallel arrangement. The (green) circles are the locations of the ether and ester groups, the (red and blue) arrows show the direction of the polarisation of the π electrons and the longitudinal dipoles.

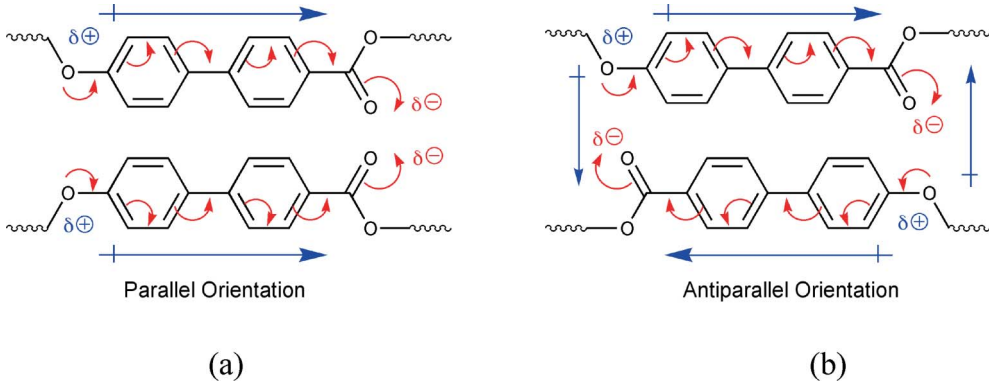

Figure 14. Polarisabilities of the core sections of butyl 4′-n-octyloxybiphenyl-4-carboxylate: (a) the parallel arrangement; and (b) the antiparallel arrangement showing the formation of a quadrupole.

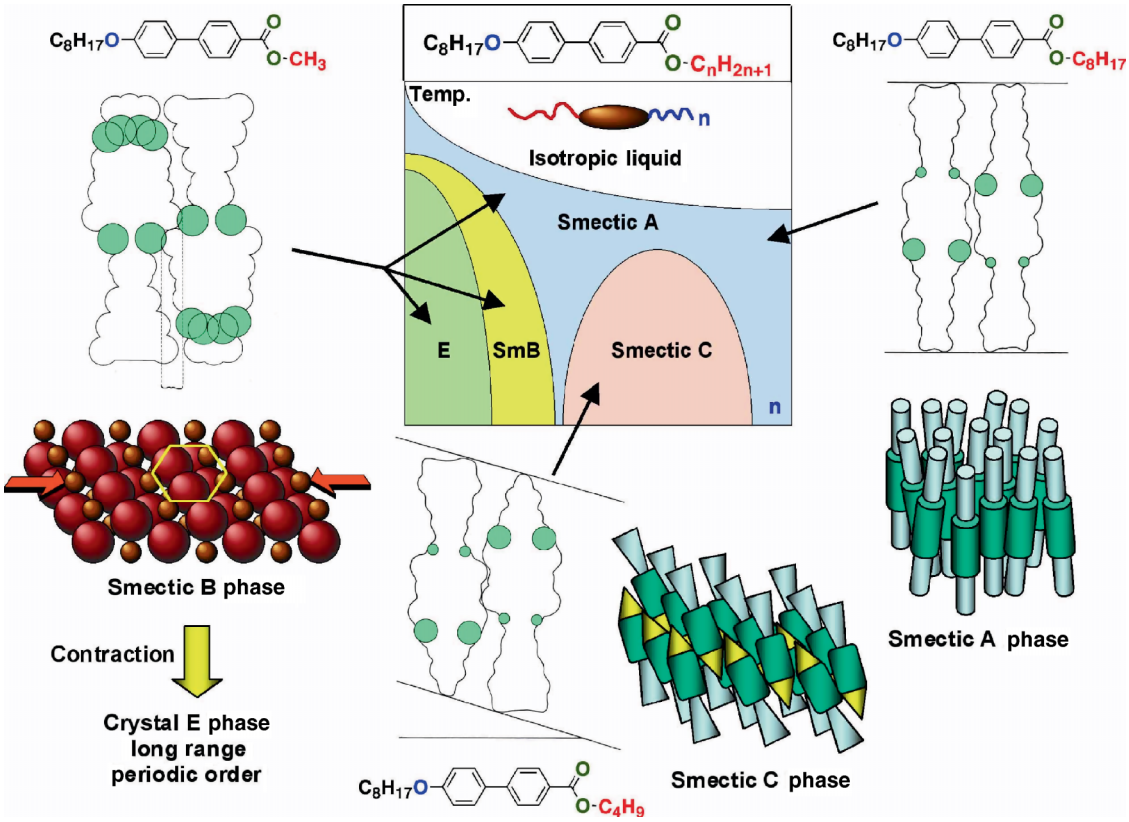

Figure 15. The phase transitions alkyl 4′-n-alkoxybiphenyl-4-carboxylates (centre). The minimised rotational structures of the methyl, butyl and octyl esters and the mesophases that they form.

homologues, quickly maximises and falls away again. Above seven carbon atoms in the ester chain the smectic A phase is the only liquid crystal phase observed. Using the same modelling methods described above in the evaluation of the architecture of octyl 4′-n-octyloxybiphenyl-4-carboxylate (See Figure 15, right) shows that the molecule has a rolling-pin three-dimensional shape. There is no advantage for this material to form tilted phases because in the orthogonal smectic A arrangement the quadrupolar interactions between the ether and ester functions are closer and therefore stronger than for the tilted arrangement. The rolling-pin shape, however, is not conducive to sharing space and so ordered smectic phases are disfavoured.

The shape of the volume of revolution for the first homologue of the series, methyl 4′-n-octyloxybiphenyl-4-carboxylate, is of a tumble-boy type (see Figure 15, left). Most of the compounds studied so far which have strong smectic B characteristics have rotational molecular shapes of the tumble-boy variety (*38*). If a molecule that has a tumble-boy rotational shape comes into close proximity with another similar molecule, then at a transition to a smectic B phase these molecules must be able pack closely together. It is known that the separation of the molecular centres in the B phase is extremely small (3–4 Å), therefore the intermolecular separation is of a magnitude whereby the space occupied by one of the molecules is partly shared by its nearest neighbour, i.e. the rotational molecular volumes are interpenetrable. In this close-packed situation, however, molecular rotation is still permitted provided it is of a coordinated nature. Therefore, even though the rotational volumes are interpenetrated, as the molecules move closer together in order to coordinate their rotational motions and form this close-packed arrangement they must pass through a situation where for some molecules the volumes themselves are closely packed. Consider the packing arrangements of the tumble-boy shapes as shown in Figure 15 (left). It can be seen that the head-to-tail orthogonal packing arrangement shows very close packing of the molecules so that they even interpenetrate each other's cylindrical volume of space without interfering with each other's rotational motion.

Having described the situation for two molecules close-packed together these ideas can be extended to groups of molecules. Consider the addition of one molecule to a closely packed pair. The next molecule can pack closely either up or down. The packing arrangement of a trio of molecules forms the basis for packing in the hexagonal matrix. Remembering

that the molecular motion in the B phase is coordinated and thus the swept out volumes are interpenetrable; the molecules can be packed together in a 'stylised' way in order to alleviate some of the coordinated motion in certain directions. The optimum packing arrangement for the tumble-boy shapes is in rows (see Figure 15, left; smectic B phase). Rotation can then occur in a well-coordinated way into the layers, but in a less well-defined fashion in the perpendicular direction along the layers, as shown in the centre left part of Figure 15. This is due to the sharing of space by the tumble-boy shapes occurring across the rows in head-to-tail arrangements. When the heads are the same way up, i.e. along the rows, there has to be a greater interpenetration of each other's space and hence the rotational motion is well coordinated. This type of packing may occur in small domains but it will become random over large areas. The subsequent transition to the crystal E phase can occur via a contraction across the rows in which the molecules have head-to-tail arrangements. Thus, the utilisation of the remaining space available, i.e. that between the head-to-tail arrangements of the volumes, aids the drive to form an orthorhombically close-packed matrix. In this case the molecules will no longer be able to rotate freely or coordinately but will only oscillate as the remaining free space is occupied

So far we can appreciate from this modelling that the early homologues exhibit orthogonal A, B and E phases, which give way to the introduction of tilted C phases, and then for the longer homologues no polymorphism is found and the A phase predominates. However, it is also possible to understand from the 'steric shape-quadrupole' model how the balance of dipolar forces, induced polarisability, shape constriction and rotational volume interpenetration can favour the formation of hexatic B, I and F phases over the stabilisation of crystal B, J, G, H, K and E phases. For example, in the series of compounds described above, the smectic B phase is a hexatic B modification and not a crystal B phase. For the molecular orientation shown in Figure 14, the *Lennard–Jones* potential energy well associated with the permanent dipolar effects coupled with the short-range repulsive interactions prevent the mesophase collapsing into a crystal-like structure with long-range translational order, hence, 4-n-hexyl 4′-n-pentyloxybiphenyl-4-carboxylate (65OBC) (see (*42*)) exhibits A, hexatic B and crystal E phases.

The polarisability of the molecular structure is another important factor to be considered in the phase formation. Removal of the source of the mesomeric relay (in this case the alkoxy oxygen atom) or the insertion of a group or atom which prevents this relay thus producing isolated dipoles will depress the liquid crystal properties of the system in some cases. Even the simple exchange of oxygen for sulphur in the ester function to give the thioester, hexyl 4′-pentyloxybiphenyl-4-thiocarboxylate (65OBTC) (see (*44*)) results in a material that exhibits a crystal B rather than a hexatic B in its phase sequence. The thioester is not as strongly polar as the ester, and hence the repulsive interactions are weaker.

4. Transmission of structural information

Up until now we have discussed complexity in terms of molecular architecture with respect to the molecular core and the peripheral chains, and the local lateral interactions between the molecules. We now turn to the issues of complexity created via the interactions between the layers in lamellar systems, where the information on the local molecular organisation within a layer is transmitted and amplified between layers.

Although the effects of lateral molecular interactions on mesophase formation have been investigated extensively through the development of property–structure correlations, terminal interactions, conversely, have not been investigated in depth because they have generally been thought not to influence mesophase stability to a great extent. As a consequence, few systematic studies have been reported where the terminal positions of the aliphatic chains have been manipulated and redesigned; however, through these limited, and unsystematic, studies there has been a realisation that small changes to the termini of the molecular structure can have a very marked effect on layered, smectic phase formation and related physical properties, particularly for synclinic and anticlinic (and related ferroelectric, ferrielectric and antiferroelectric) phases. Moreover, the understanding of the interactions at, and between, the interfaces of the layers in lamellar smectic phases is of practical importance in the development of ferroelectric devices and displays (*45–47*).

There are a number of interactions to consider in respect of devices which include the liquid crystal surface interactions, the penetration of the surface interactions into the bulk of the liquid crystal phase, the strength of the lateral interactions between the molecules and the strength of the interactions between the layers, as shown in Figure 16. The strength of the surface interactions control the surface anchoring energies and hence the bistability of the device operation. The strength of the interactions between the layers controls the shape of the hysteresis loop for the ferroelectric phase. Weak interlayer (out-of-plane) interactions can lead to a collapse of the hysteresis loop, and hence these can markedly affect device configuration, construction and performance (*48*). For example, weak interlayer interactions leading to the collapse of the hysteresis loop results in a linear

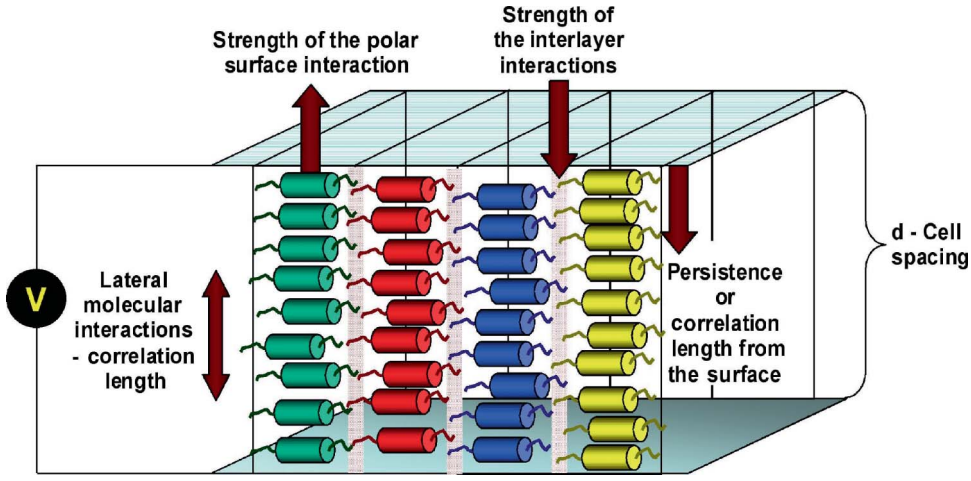

Figure 16. A typical device arrangement for smectic liquid crystals, with the layer planes perpendicular to the cell surface. The important intermolecular and surface interactions are shown by the block arrows.

electrooptic response to an applied electric field (V-haped switching), thereby enabling the device to exhibit a greyscale response suitable for video-frame rate applications (*49*).

The interactions between the layers in smectic liquid crystals can be affected by including a substituent in the terminal position of one or both of the flexible chains. The substituent can be either sterically encumbering or polar or a combination of both. If we consider first the inclusion of one terminal group to give the molecular design shown in Figure 17, then the number of possible isomers is 16, twice the number for a mesogen without a terminal group.

Although the incorporation of one terminal group can lead to a number of isomers being possible, it can of course also lead to a variety of novel mesophases being formed. For example, the diagrams in Figure 18 show a comparison between how a normal smectic layer might appear (Figure 18(a)), and how the interlayer organisation might appear with the incorporation of bulky or chemically dissimilar groups, shown as discs, at the terminal positions of the structures in the molecules. For Figure 18(b) we have drawn the structure of the mesophase with as many molecules pointing up as there are down and homogeneously distributed within the layer. Structural variations could exist at one extreme with clusters of up and down molecular species forming an inhomogeneously ordered system e.g. rafts (Figure 18(c)), right through to fully two-dimensional modulated structures (Figure 18(d)). All of these arrangements would, of course, have profound effects on mesophase

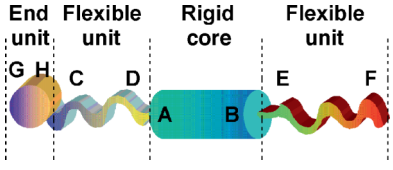

Figure 17. Molecular design of a mesogen possessing one sterically encumbering or polar terminal group.

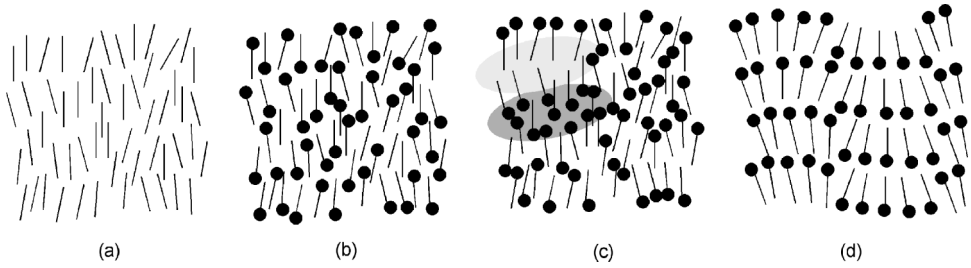

Figure 18. (a) The disorganised layer structure of a typical smectic A liquid crystal with the molecules shown as rods. (b) The disorganised layered structure of a smectic A liquid crystal where the molecules have bulky encumbering or polar end groups. (c) Clustering of tails and head groups (rafts) to give an inhomogeneous layer structure (highlighted in grey). (d) In-plane ordering of the molecules caused by the induced curvature of the packing of the end groups together; the modulation may be one-dimensional or two dimensional within the layer.

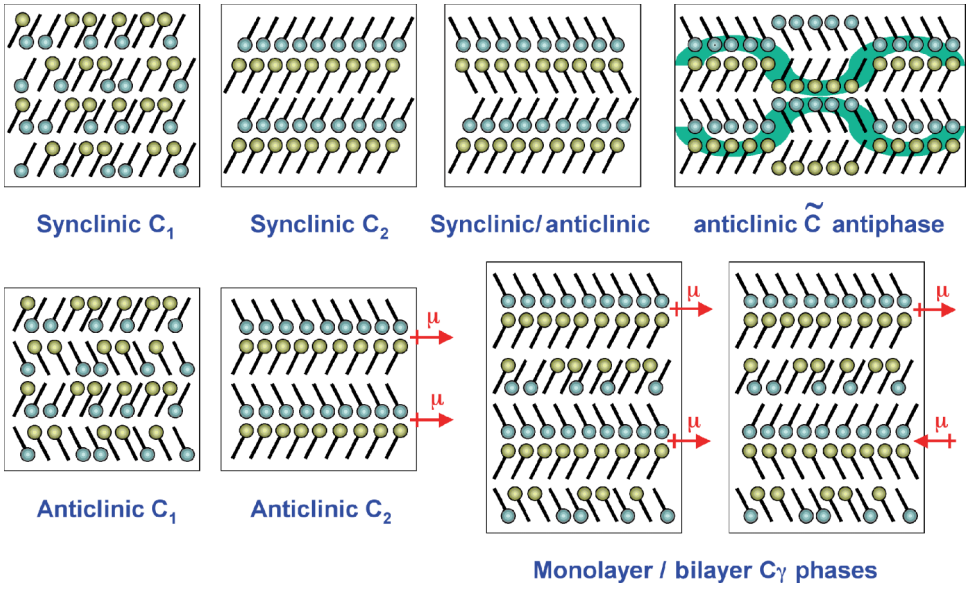

Figure 19. Potential structures for mesophases where the molecules have structures that possess a polar or sterically encumbering terminal group (shown as (blue and yellow) spheres) and are tilted with respect to the layer planes.

formation, the arrangements of the molecules in their layers, and the ensuing physical properties.

When mesophases based on layered structures are formed, where the molecules are tilted with respect to the layer planes, a greater number of variations become possible (*50*). The varieties can be based on synclinic, where the tilt direction from layer to layer is maintained, or anticlinic, where the tilt direction alternates from layer to layer orientations, as shown in Figure 19. Mixed synclinic and anticlinic layer structures form the basis of ferrielectric ordering in chiral systems. In Figure 19 the terminal groups attached to the flexible aliphatic chains are shown as spheres and the rest of the molecules are shown as rods thereby over-emphasising the role of the terminal groups in the packing arrangements of the molecules. Monolayer smectic C_1 synclinic and anticlinic mesophases and bilayer C_2 synclinic and anticlinic modifications are possible. In-plane modulated structures and ferrielectric phases are also shown as possibilities.

4.1 *Polar versus non-polar interlayer interactions*

We now turn to examples of synthesised materials possessing polar or sterically encumbering end groups and compare the mesophase formation with examples of materials, shown in Section 2, that do not possess such an end group. In this case the examples are based on mesogens having difluoro-substituted terphenyl cores. Figure 20 (right) shows a systematic study for polar (halogeno) terminal group structure/property correlation in difluoroterphenyls. All of the molecular structures, except for the terminal groups, are kept the same. The figure lists a number of compounds where a halogen atom has been located at the terminal position. In comparison to the materials with straight aliphatic chains, which exhibit nematic, smectic A and synclinic smectic C phases, the terminal halogeno compounds exhibit only smectic A phases. So in other words the substitution with a halogen has the effect of suppressing nematic phase formation and inducing the molecules to stand up in the smectic layers rather than allowing them to tilt over. This may be due to strong polar interactions at the layer

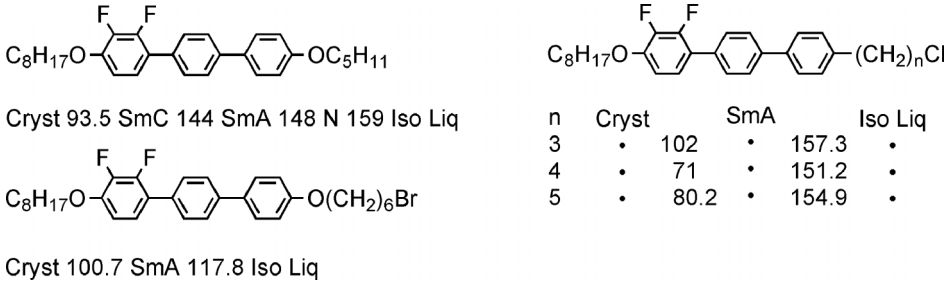

Figure 20. Mesophase phase behaviour of difluoro-substituted terphenyls which carry a polar terminal halogen.

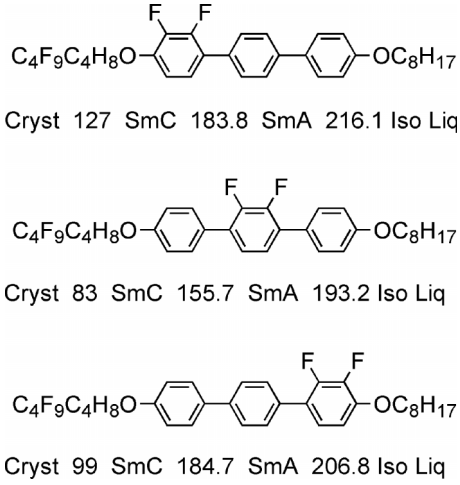

Figure 21. Effect on mesophase formation and transition temperatures (°C) of the incorporation of a fluorocarbon chain at the terminal position in difluoro-substituted terphenyls.

interfaces caused by the terminal halogens. So in the first instance it appears that we can control molecular tilt via the fine-tuning induced by changing one atom (halogen for H) at the layer interface.

Conversely, however, when the terminal substituent is a short fluorocarbon chain, the tilted smectic C phase returns, but again nematic phases remain suppressed. Figure 21 shows the transition temperatures for three homologues where the only difference between the three is the location of the fluoro-substituents associated with the aromatic core. If these results are compared with the transition temperatures determined for similar difluoro-substituted alkyl-alkoxy terphenyls, shown in Figure 8, and the dialkyl difluoroterphenyls, shown in Figure 9, it can be seen that for the alkyl terminated homologues with the two fluorine substituents located on the middle ring, both nematic and smectic C phases are found, whereas the equivalent material with a terminal fluorocarbon chain exhibits smectic A and smectic C phases. Thus, although the materials possessing terminal carbofluoro-chains exhibit smectic C phases, they also have strong tendencies towards the formation of orthogonal phases and not to disorganised phases such as the nematic phase. Consequently, similarly to the terminal halogeno-materials shown in Figure 20, the terminal fluorocarbon substituted homologues favour orthogonal phases, indicating that strong polar interactions at the interlayer interfaces have a marked effect on mesophase formation irrespective of the lateral interactions of the terphenyl core units.

Polarity can also be introduced into the terminal chains via the incorporation of ether linkages in the form of ethyleneoxy units. Figure 22 shows a family of materials where the number of ethyleneoxy units has been sequentially increased in number (left-hand column) (*47*). This family of materials all exhibit nematic, smectic A and smectic C phases. Interestingly, the transition temperatures fall as the number of ethyleneoxy groups rises, indicating that even though the polarity along the aliphatic chain is being increased, which might be expected to increase the strength of the lateral interactions, the increased strength of the hard core polar repulsions suppresses liquid crystal phase formation. The right-hand column shows that introducing a lateral methyl group into the ethyleneoxy unit has the surprising effect of suppressing the formation of the smectic A phase. The lateral methyl groups possibly weaken the polar interactions because of steric repulsion. Similarly, extending the number of methylene units between the oxygen atoms, thereby reducing the degree

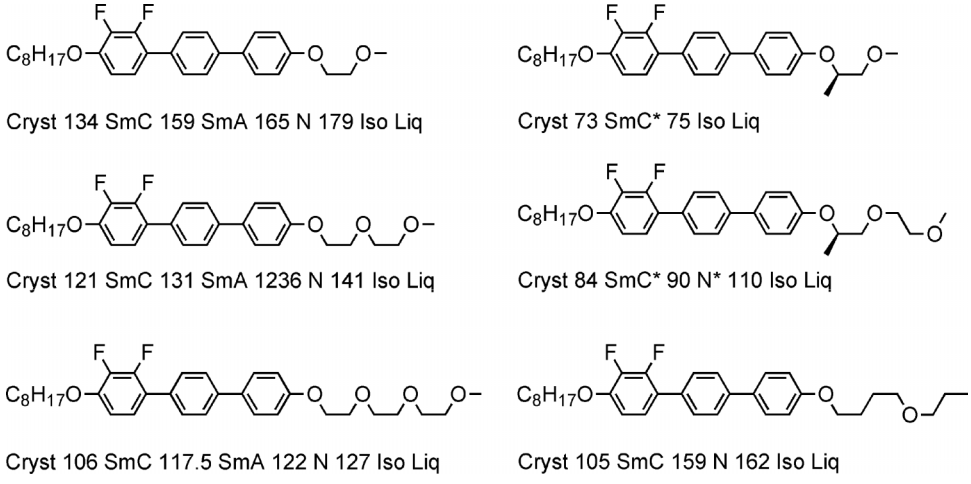

Figure 22. Effect on mesophase formation and transition temperatures (°C) of the incorporation of an ethyleneoxy chain in difluoro-substituted terphenyls.

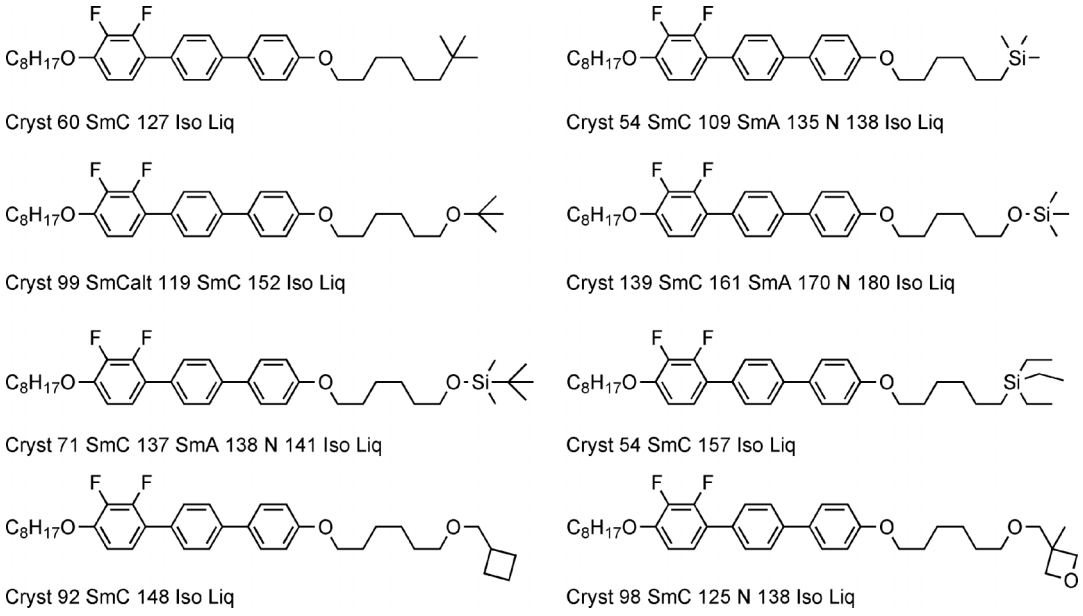

Figure 23. Effect on mesophase formation and transition temperatures (°C) of the incorporation of silyl, siloxane and ether units at the terminal position in difluoro-substituted terphenyls.

of polarity, has the same effect of lowering the polarity. Thus, these studies demonstrate that the stronger the polarity in the terminal chain, the more likely it is that a material will exhibit an orthogonal smectic A phase.

The polarity at the terminal position can also be varied by incorporation of a terminal silane unit for comparison with a terminal ether. Figure 23 shows a comparison between terminal silanes, siloxanes, ethers, and cyclic ethers [47]. All of the materials were found to exhibit synclinic smectic C phases. However, for one compound, the tertiary butyl ether, an anticlinic phase as well as a synclinic phase was found. Conversely, all of the materials with terminal silicon based groups suppress the formation of anticlinic phases, and a number of compounds exhibit N, smectic A and smectic C sequences. It is remarkable that these materials exhibit nematic phases, as it is unusual for compounds with terminal silicon containing groups to do so. Typically materials with siloxane terminal groups do not exhibit nematic phases, and usually have properties more in keeping with direct smectic C to liquid transitions. If the materials with polar terminal ethers are compared, it can be seen that the end groups with higher polarity induce the formation of nematic phases and often with the exclusion of smectic A phases. Overall, most of the materials that have terminal groups possessing exposed heteroatoms, i.e. not crowded with aliphatic chains tend to exhibit nematic phases.

The use of siloxane and silane terminal end groups provides a route to novel materials which are not composed solely of carbon, hydrogen, oxygen and nitrogen. Typically for nearly all of the materials we have investigated, those bearing terminal siloxane groups exhibit smectic C phases with very few possessing smectic polymorphism. For nearly all of the materials, the tilt angle in the smectic C phase was found to be relatively high, usually in excess of 30°. In the design of such materials it is often common to vary the methylene spacer chain length linking the siloxane unit to the aromatic core of the material. Although it is possible to have multiple SiO units in the terminal group, commonly units possessing either two or three silicon atoms are the norm. Figure 24 shows the variation of the transition temperatures for a family of disiloxane-substituted difluoroterphenyls [51]. All of the materials exhibit smectic C phases with clearing points near to 130°C and melting points in the range of 55 to 80°C. In addition, there appeared to be little influence on the clearing points of the change in methylene spacer chain length; however, as expected, the melting points varied

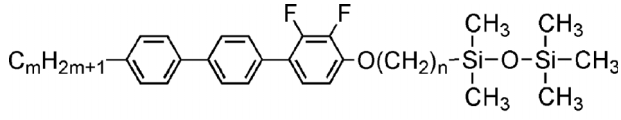

m	n	Cr		SmC		Iso Liq
5	5	•	57.4	•	136.5	•
5	7	•	70.0	•	139.2	•
7	5	•	76.3	•	129.6	•
7	7	•	62.7	•	132.2	•

Figure 24. Effect on mesophase formation and transition temperatures (°C) of the methylene spacer chain length (*n*) on silyloxy-substituted difluoro terphenyls.

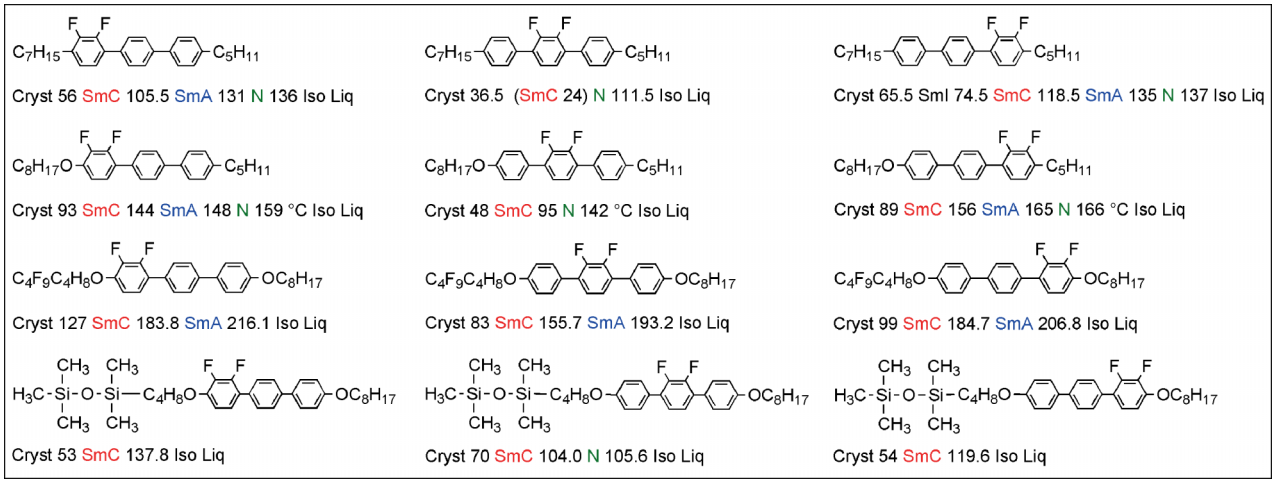

Figure 25. Comparison of the mesophase phase sequences and transition temperatures (°C) with respect to the positions of the fluoro-substituents in difluoroterphenyls relative to the types of terminal chains/functional groups.

greatly. Nevertheless, the materials are of practical interest as host systems in ferroelectric mixtures.

If we compare transition temperatures and phase sequences with respect to the positions of the fluoro-substituents in terphenyls relative to the natures of the terminal chains, i.e. dialkyl, alkyl-alkoxy, alkoxy-fluoroalkyl and alkoxy-silyloxy, as shown in Figure 25, some fascinating structure–property correlations are revealed. First, only the dialkyl materials exhibit any of the more ordered smectic phases; the silyloxy-terminated materials strongly favour smectic C phases; the materials with the fluoro-substituents in the centre ring strongly favour nematic phases; and the materials with fluorocarbon end groups disfavour nematic phases but strongly favour smectic A phases and have the highest mesophase thermal stability. In addition, the more complicated the molecular structure is (e.g. the silyloxy materials), the less complex the mesophase behaviour.

If the results on the melting behaviours of the silyloxy terminated difluoroterphenyls are compared with analogous materials but with terminal silane units, the melting and clearing points are similar, with the materials again favouring the formation of smectic C phases, see Figure 26 (see also (*51*)). Smectic A phases, this time, only appear for fairly long aliphatic terminal chains and methylene spacer units. Thus, in this case the smectic A phase does not appear due to polarity in the terminal chain, as in the fluorocarbon terminated systems, but because the aliphatic chains are starting to dominate the interactions over those of the aromatic core.

So far we have only discussed the use of conventional terminal groups in molecular design. However, mesogenic moieties that are to be grafted onto a polymer backbone or tethered to a dendritic scaffold or a

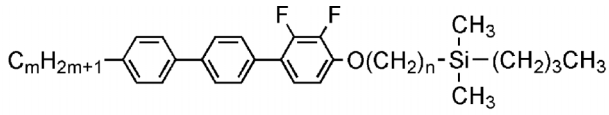

m	n	Cr		SmC		SmA		Iso Liq
5	5	•	61	•	129	-		•
5	7	•	60	•	130	-		•
7	5	•	60	•	123	-		•
7	7	•	65	•	122	•	125	•

Figure 26. Effect on mesophase formation and transition temperatures (°C) of the methylene spacer chain length (*n*) on silyl-substituted difluoro terphenyls.

nanoparticle often provide a rich source of novel low molar mass liquid crystals with unusual end units. For example, Figure 27 shows three difluoroterphenyls with terminal groups that possess a phosphorus atom and which are designed to be attached to a magnetic nanoparticle. As with the other materials described in this section, smectic C phases appear to predominate irrespective of the locations of the two fluoro-substituents. However, the transition temperatures for the phosphates are relatively high, particularly in comparison with the silicon-containing materials described previously. This is probably due to hydrogen bonding occurring at, and possibly across, the interfaces of the layers. When the possibility of hydrogen bonding is suppressed, as for the diethyl substituted material shown in the bottom of Figure 27, the transition temperatures are lowered and a nematic phase is introduced. Thus, terminal interactions between the molecules raises transition temperatures, stabilises layered structures (particularly the smectic C phase) and suppresses nematic phases, whereas reducing the terminal interactions lowers the stability of

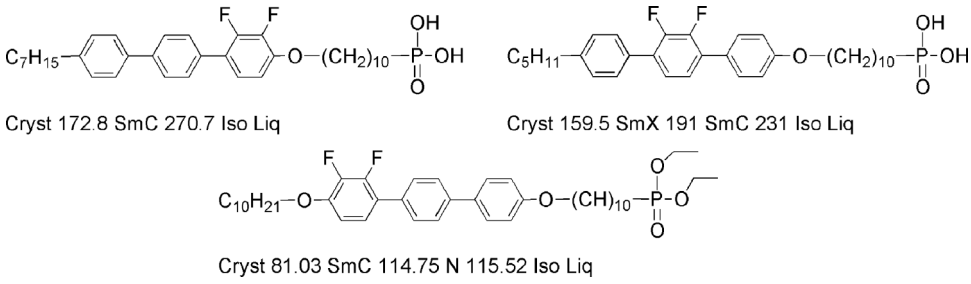

Figure 27. Effect on mesophase stability and transition temperatures (°C) on three terminally substituted difluoro terphenyls.

layered phases and introduces the disordered nematic phase; however, the smectic C phase is still favoured.

Overall, these studies, along with all of the others on terminal group variation favour tilted lamellar phases over nematic and orthogonal lamellar phases.

4.2 Synclinic versus anticlinic ordering and terminal chain angle dependency

When a material forming a synclinic (tilted) phase, i.e. where the tilt direction of the molecules propagates from layer to layer, is chiral, then the mesophase becomes ferroelectric (P_s is finite), and when it forms an anticlinic structure the phase becomes antiferroelectric ($P_s = 0$). Controlling the molecular tilt directions between layers thus becomes particularly important for the development of fast switching devices. It has been found that the local director can be controlled from layer to layer through judicious design of the terminal end groups. Most notably, the orientation of the terminal group, i.e. its presentation to adjacent layers, and its ability to interact with the neighbouring layer are the important factors in determining the tilt orientation on passing from one layer to the next in a bulk sample of the material (*50*, *52–56*). Furthermore, Bartolino *et al.* (*57*) demonstrated that the molecules in lamellar phases, which generally have zig-zag shapes, are oriented within the layers so that the cores are more tilted than the tails with respect to the layer planes. In this way the terminal groups of the flexible end chains are presented so that they are almost perpendicular to the layer interfaces, and thus are able interact with, and even interpenetrate, the adjacent layers. Therefore, the angle of the presentation of the termini of the flexible units is potentially an important factor in determining mesophase formation. Indeed, there have been many representations of terminal chains being spread out along the interfaces between layers in anticlinic phases as a rationale for the formation of antiferroelectric mesophases (*58*), as shown in Figure 28. This postulation, however, is erroneous because it does not take into account the packing volume and associated constraints with respect to the dynamic motions of the molecules.

However, consider the terphenyls shown in Figure 29. All of the materials have the same structure except for the right-hand terminal chain (*59*). The left-hand column has attachments of the right-hand group via an ether linkage (**a** and **b**), whereas for the right-hand column the attachment is through an ester unit (**c** and **d**). As a consequence the terminal groups of the ethers are set at a smaller angle with respect to the rigid core than for the esters. This means that for zig-zag shaped molecules, the angles by which the terminal groups are presented to the layer interfaces are different, with the terminal groups of the esters being presented almost perpendicularly with respect to the layer planes, whereas those for the ethers being presented at an angle. As shown for **a** and **c** in Figure 30. The consequence of this is that the interfacial interactions are weakened in the case of the ethers relative to esters, which results in greater stabilisation of the nematic phase relative to lamellar phases, and subsequent lowering of the stabilities of orthogonal phases, and an increased stability of synclinic over anticlinic ordering. In essence, the ethers tend to be more disruptive to layer formation than the esters, which tend to promote it (*60*).

The relationship between terminal ethers and esters in their abilities to form synclinic versus anticlinic phases has been known for many years; however, this work was mostly confined to the study of the properties of biphenyl-4-yl-carbonyloxy benzoates (*61–63*), which are not stable for practical devices such as projection displays. Difluoroterphenyls, on the other hand, are very stable materials with suitably desirable physical properties for use in ferroelectric applications. However, without the use of terminal controlling groups it is very difficult to induce the formation of anticlinic phases in these materials. Through the judicious choice of various terminal groups it has become apparent that a wide variety of mesophase types and sequences can be controlled by this methodology, and indeed under certain circumstances novel phases and phase behaviour have been observed, such as re-entrancy (*64*).

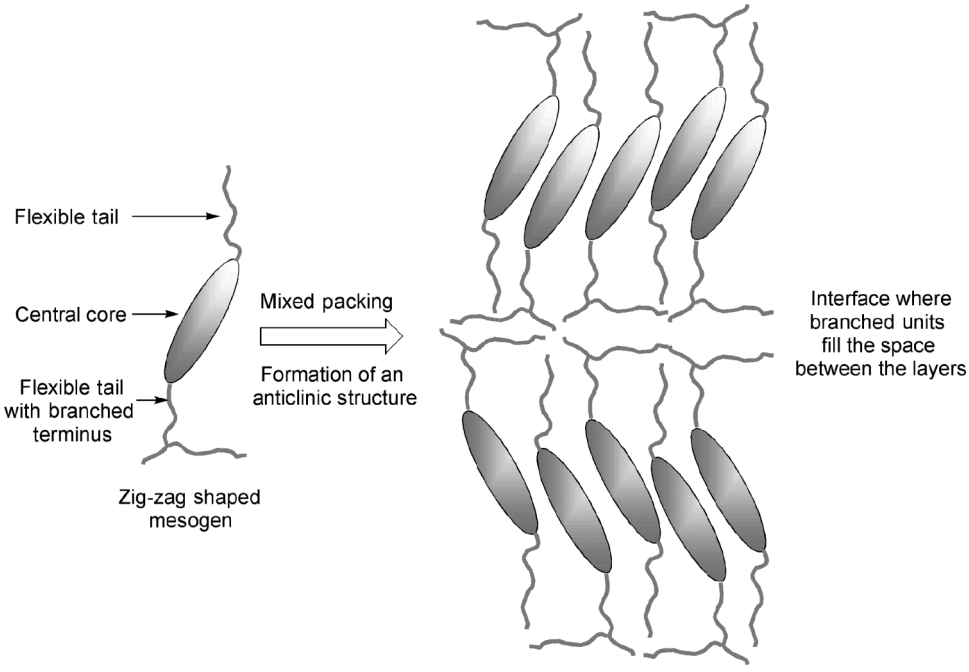

Figure 28. Proposed interaction between the layers in anticlinic ordered liquid crystals.

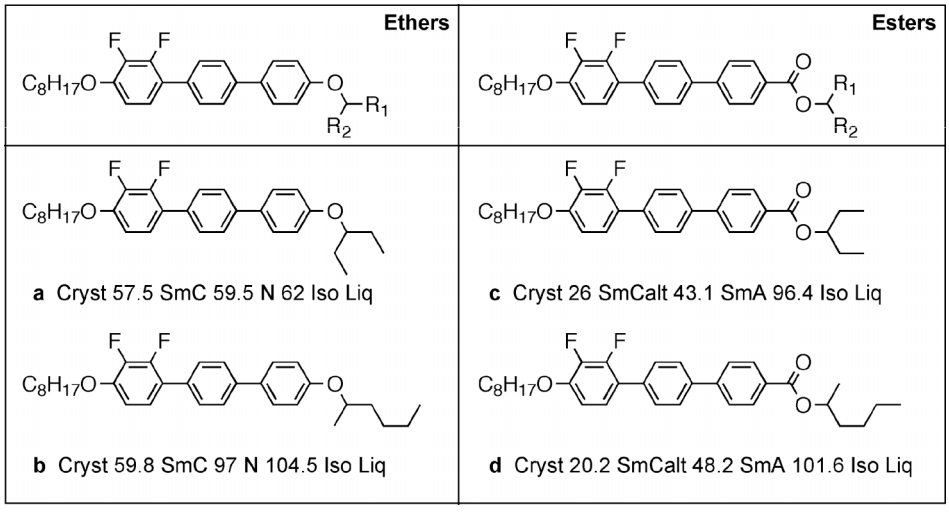

Figure 29. Comparison of transition temperatures (°C) and mesophase sequences of difluoro-substituted terphenyl ethers versus the analogous esters.

A zig-zag molecular shape implies that mirror symmetry exists down the long axis of the structure; however, as soon as a stereogenic centre is introduced into the structure, typically in the terminal chain, the symmetry is broken. Thus, if the stereogenic centre is located adjacent to the central core the orientation of the terminal chain relative to the core and opposing terminal chain is somewhat fixed, as shown in Figure 31. The side-on orientation suggests a zig-zag shaped gross structure; however, the end-on orientation demonstrates that the molecular structure is not rod-like, or zig-zag shaped as shown in the right-hand structure in the figure, or even banana-like (as utilised in many theories), but 'twisted' as depicted in the diagram in the left-hand part of the figure.

The molecular twist, thus, is essentially caused by the stereochemistry about the chiral centre. The degree of the internal 'molecular twist' will be proportional to (i) the molecular length, (ii) the angles that the chains make with the core, (iii) the rotational distribution functions of the terminal chains, the core and the overall molecular structure and (iv) the stereochemistry

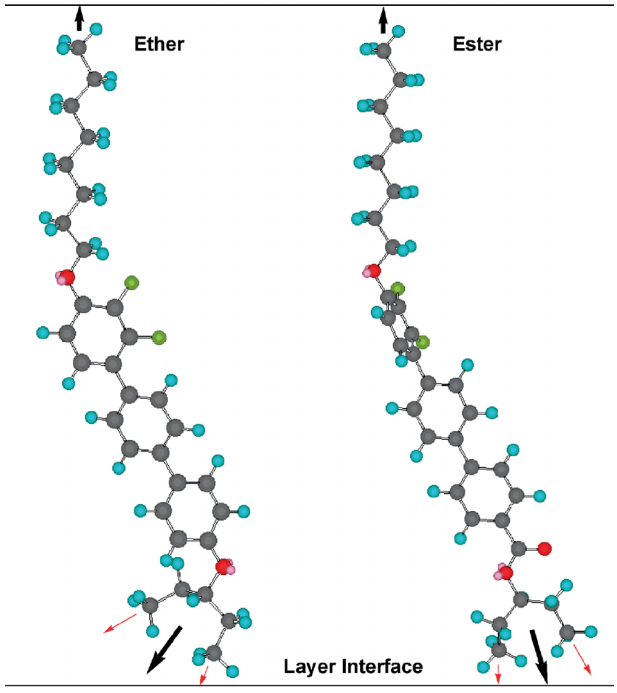

Figure 30. Presentation of the terminal groups at the layer interfaces in tilted smectic phases.

and location of the chiral centre relative to the core and the length of the terminal chain. If we assume that the molecules are fixed, i.e. are not in dynamic motion, then a simple or crude way of describing the molecular twist is through the displacement, α, of the end of the molecular structure relative to the racemate, as shown in Figure 31. The displacement will increase if the molecular length is increased or if the distribution functions for the various molecular rotations are rotationally damped. The displacement in some senses is therefore a measure of the degree of breaking of the mirror symmetry of the system.

Now consider how molecules with twisted structures pack together in the tilted smectic C* phase. The molecules will be packed in a random head-to-tail arrangement within the layer, and there will be substantial interlayer mixing of the molecules at the interfaces between the layers. Thus, the molecular twist will be passed from one layer to the next as described by Yoshizawa *et al.* and Bartolino *et al.* (*55–57*). As a result the tilt directors of the molecules will be rotated on passing from one layer to the next, thereby forming a helix.

The pitch of the helix will be determined by the tilt angle θ, the molecular length l and the displacement α.

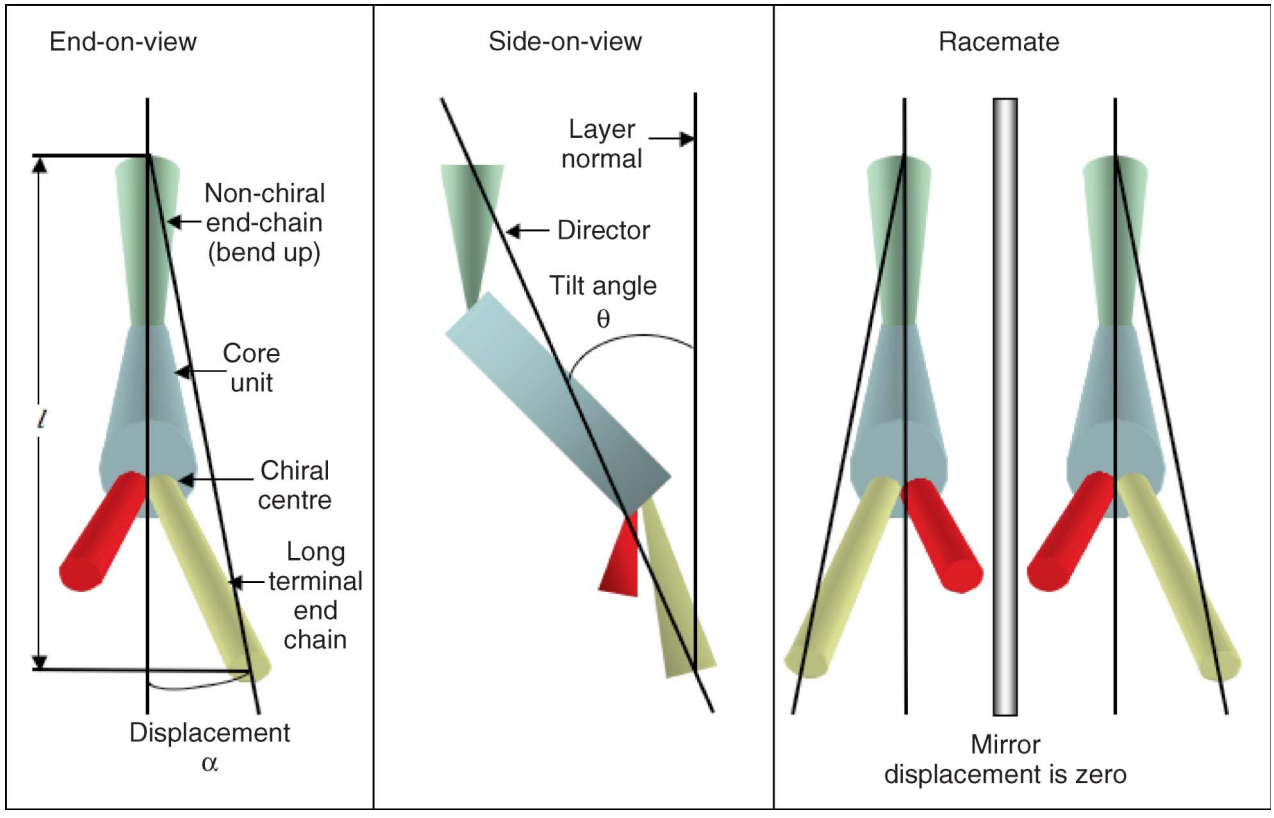

Figure 31. The twisted structure of a chiral mesogen where the asymmetric centre is located near to the central core thereby preventing rotation disordering.

The helical structure could, therefore, be envisaged as being a result of a three-dimensional molecular twist being superimposed upon the periodic two-dimensional interfaces of the layers. The helix direction will be determined by the molecular twist which itself is related to the stereochemistry about the chiral centre, the location of the chiral centre within the molecular structure and the zig-zag orientation of the molecule, i.e. it will be related to the empirical property–structure correlations developed in earlier studies (*65*).

Thus, by reducing the freedom of motion by judicious choice of the location of the stereochemical centre, the distribution of conformers will also reduced which has the effect of fixing the shapes of the molecules. One could almost imagine that when the motion about the stereogenic centre is relatively free the molecule will appear as a blur, but when it is reduced the molecule will come into sharper focus. As a consequence of the reduced rotational freedom the degree of broken symmetry and the molecular twist are enhanced. This means that for molecules that have better-defined shapes, the molecular twist will be transmitted between layers more efficiently.

For materials with large values of l and α, and which exhibit tilted phases, the system will twist up tightly to give short pitch phases. However, there will come a point where the twist induced by the twisted molecular structure cannot be sustained because the ends of the terminal chains will meet the layer interfaces at a shallow angle, thereby causing the layers to bend with respect to one another. Thus, for small molecular twists the ensuing helical arrangement of the molecules is a low-energy escape mechanism, whereas for large molecular twists the resulting helical structure is high energy, and therefore in this situation a compromise becomes possible. The system would prefer to have a helical structure but with a longer pitch. This can be achieved by having alternating tilting of the molecules on passing from one layer to the next, as in the proposed structure of an antiferroelectric phase. Figure 32 shows this structure for twisted molecules. Immediately it becomes apparent that by having back-to-back layer tilts the pitch of the helical structure is lengthened, and the pressure to form a twisted structure is greatly reduced. This structural transformation provides an escape from the system producing a high-energy helical state. Thus, a frustration is produced between the desire to twist and at the same time to maintain the layered ordering of the phase.

Not surprisingly, therefore, materials that exhibit antiferroelectric phases tend to have chiral centres that are adjacent to the central core region of the molecule, have long aliphatic chains attached to the chiral centre, and have long central core regions. Molecules with

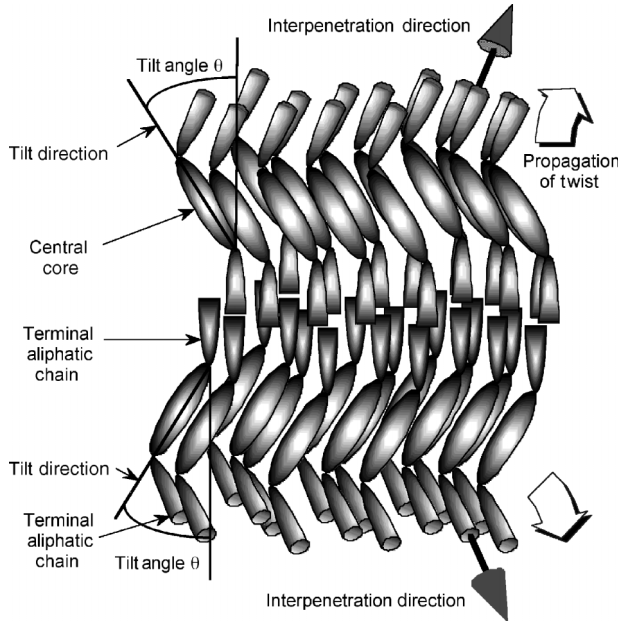

Figure 32. Anticlinic arrangement of chiral molecules with twisted molecular structures that self-organise to form an antiferroelectric phase.

these structural attributes will have high populations of certain preferred conformations, have better-defined zig-zag bent shapes, high molecular twists and as a result will be candidates for frustration to occur between helical twist and layer rotation. In addition, it is known that antiferroelectric phase can be exhibited by materials where the chiral centre is not adjacent to the central aromatic core; for such materials, however, it is common that the second aliphatic chain possesses a terminal end group and a spacer chain length (odd in number overall) that is conducive to anticlinic ordering (*66*).

Furthermore, the effect that the peripheral aliphatic chain length has on the phase behaviour of materials that have molecules with twisted structures can be described in the following way. For short chains there will be little effective twist and weak interlayer permeations and so antiferroelectric phases will be unlikely to occur. For very long peripheral chains, the chain ends (maybe the last few carbon atoms in the chain) will have a high degree of mobility and freedom of rotation. Therefore, effective interlayer permeation will be reduced by the end chains bending, flexing and even doubling back on themselves. Therefore, antiferroelectric phases would not be expected to be found for such long chain lengths (i.e. C_{18}+). Consequently, antiferroelectric phases are most likely to occur at intermediary chain lengths where the aliphatic chains are long enough and inflexible enough to convey the molecular twist between layers.

In the modelling of antiferroelectric phases, it is interesting to compare the effects of extending the length of the lateral aliphatic chain at the chiral centre (methyl to ethyl to propyl). It has been shown that the antiferroelectric phase becomes stabilised as the lateral chain length is increased (*52*). We could extend this chain to a point where the two terminal chains at one end of the molecule have the same length, and the system is no longer chiral and therefore does not form a helical macrostructure, as described earlier. A swallow-tailed material will show an alternating tilted arrangement of the layers, but this is expected as now there are two equally matched interlayer permeations to consider for each of the terminal chains of the swallow end of the molecule. Thus, chiral materials can be anticlinic and antiferroelectric, and achiral materials can be anticlinic even though they are not antiferroelectric, and consequently it can be assumed that minimisation of the spontaneous polarisations associated with the alternation of the tilts is not the primary force driving the formation of antiferroelectric mesophases as suggested (*58*). There is further circumstantial evidence for this postulation which comes from the fact that achiral systems do not exhibit ferrielectric phases, because these phases are stabilised by twist and not polarity.

4.3 Conformational structures, clustering and inversions of chiral properties

The complexity in layered systems can be further complicated by the introduction of conformational variants. In systems with large molecular structures, conformational changes may be relatively slow in comparison to those experienced by systems with somewhat smaller molecular architectures. For large systems, variations in mesophase transition temperatures and phase type may be experienced where kinetic processes compete with those of thermodynamic processes.

However, for relatively simple systems competition between conformers and rotational species has been shown to occur through inversions of the spontaneous polarisation or their associated pyroelectric properties. For example, *S*-2-methylbutyl 4′-alkanoyloxybiphenyl-4-carboxylates and *S*-2-methylbutyl 4′-alkenoyloxybiphenyl-4-carboxylates exhibit an inversion in the polarisation direction in their ferroelectric phases as a function of temperature, see Figure 33 (see also (*67*, *68*)). At the crossover point the polarisation will become zero and the helical unwinding voltage increases sharply as it becomes dependent solely on the dielectric anisotropy. In addition, the measured tilt angle also falls to zero, see Figure 34 for selected homologues of the *S*-2-methylbutyl 4′-alkanoyloxybiphenyl-4-carboxylates. These phenomena have been ascribed

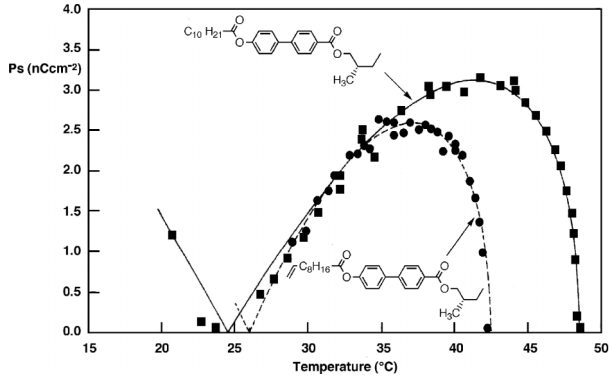

Figure 33. The spontaneous polarisation (nC cm^{-2}) measured as a function of temperature (°C) for *S*-2-methylbutyl 4′-decanoyloxybiphenyl-4-carboxylate (■) and *S*-2-methylbutyl 4′-ω-octenoyloxybiphenyl-4-carboxylate (•). The data points show experimental results, whereas the lines and dotted lines are the theory fitted to the data.

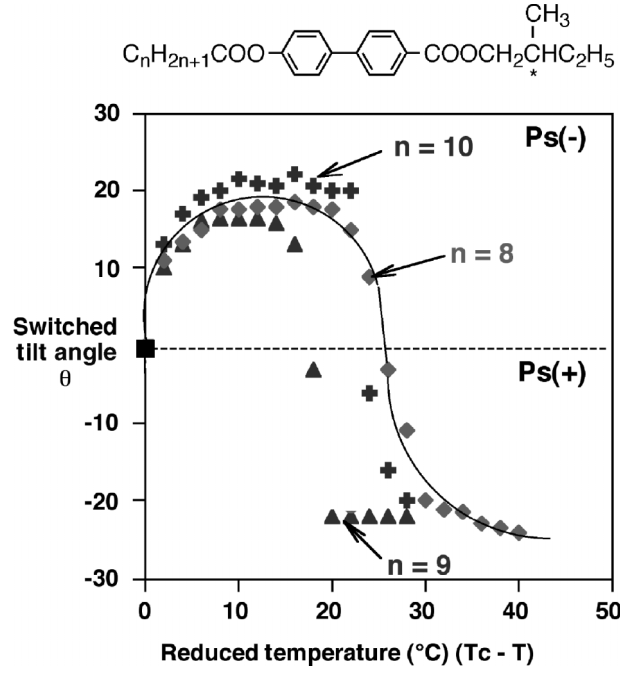

Figure 34. The tilt angle (°) determined from electrical field studies for the *S*-2-methylbutyl 4′-alkanoyloxybiphenyl-4-carboxylates as a function of the reduced temperature from the Curie point.

to changes in the distribution function of rotational species and conformers in the condensed ferroelectric phase. Thus, for a single homogeneous species

$$P_s(T) = P_o(T_{A-C} - T)^{\beta}.$$

However, if we now consider the contributions from different competing species, collectively identified as A and B, which have opposing properties, so that

$$P_s(A) \neq P_s(B)$$

for a fluctuating system there will be a dynamic equilibrium when

$$\chi(A)P_s(A) = \chi(B)P_s(B),$$

which will occur at defined temperature T for the crossover of the P_s direction and thus

$$P_s = 0.$$

However, the polarisation is a function of the dipole density, therefore

$$P \propto \Sigma_i < \mu_i > \mathrm{N}_i$$

for two interconverting species *i* and *j*, with an activation energy between the two species of $\mathrm{E_{ij}}$

$$\mathrm{N}_i = \Sigma_j \exp(-\Delta E_{ij}/kT) \,/\, V\Sigma_i\Sigma_j \exp(-\Delta E_{ij}/kT).$$

Assuming that a temperature dependence takes the form of

$$P_s \propto (T_c - T)^{\beta}$$

then, generally as the polarisation for one species (e.g. *i*) is given as

$$P_s = [\Sigma_i < \mu_i >](T_c - T)^{\beta}$$

for the two species A and B the total polarisation is found to be

$$P_s = [P_A e^{-\Delta E/kT} + P_B(1 - e^{-\Delta E/kT})](T_c - T)^{\beta}.$$

The above analysis makes no attempt to identify the nature of the competing species, other than to say there could be a collection of species with a particular polarisation direction in competition with another species of opposite sign and where the two species interconvert as a function of temperature. In terms of real systems it is possible that the interconversions are related to conformational flipping about the chiral centre, where the polarity associated with the stereogenic unit is coupled to that of the molecular dipole and hence the polarisation direction. Figure 35 shows two possible conformations, *A* and *B*, associated with the *S*-2-methylbutyl chiral end chain of (*S*)-2-methylbutyl 4′-octylanoyloxybiphenyl-4-carboxylate, where the donor methyl group at the chiral centre affects the direction of the polarity along the C_2 axis.

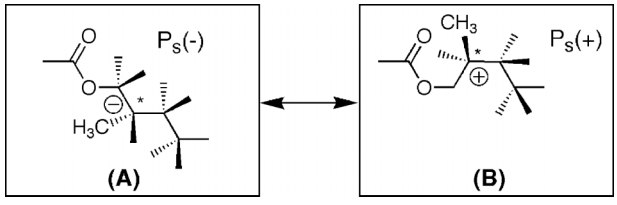

Figure 35. *Trans* and *gauche* structures which have opposing polarisation directions.

An ensemble of conformational species *A* and *B* is displayed in the diagram shown in Figure 36. Simulations of similar systems have since been reported by a number of groups on chiral nematic and smectic C* inversions, coming to similar conclusions that there are competing species which ultimately determine pitch length/polarisation direction in chiral liquid crystals (*69*).

The early theories of liquid crystallinity assumed that the molecules would 'swarm' together to form a mesophase (*70*); however, this picture was subsequently superseded by the continuum elastic theory. The inversions of chirality in nematic and ferroelectric phases resurrected the idea that molecular clustering may be important in certain phase behaviours of liquid crystal phases as described recently in relation to the swarm theory by Goodby *et al.* (*60*). The extent of the clustering, i.e. the numbers of molecules constituting a cluster, was investigated by Glass *et al.* (*71*) who studied the pyroelectric behaviours of the *S*-2-methylbutyl 4′-alkanoyloxybiphenyl-4-carboxylates. They demonstrated that the model developed for competing species could be used to determine cluster sizes, which were found to be of the order of a few hundred molecules, values that appear to be reasonable.

Inversions have also been found in chiral nematic phases, but this time with respect to the helical twist direction as a function of temperature, see the materials shown in Figure 37. At high temperature both of these compounds exhibit left-hand helical structures, but as the temperature is lowered they pass through a point where the local symmetry is still broken, but the value of the pitch reaches infinity. At this point the twist direction inverts and the helical structures become right-handed. Watson *et al.* (*69*) used a similar model to that proposed for spontaneous polarisation inversions to describe the inversion phenomena. However, in this case they resorted to solely using fluctuating conformers, rather than conformers and rotational species, to describe the inversion behaviour. Conformational modelling and molecular simulations have been used in recent years by Neal and co-workers (*72–75*) to describe inversions, and although not explicit there is an indication that local molecular architecture could be important in inversion phenomena.

5. Terminal functional groups in both flexible chains: reactive mesogens

There are many, many examples of mesogenic materials possessing functional groups at the terminal

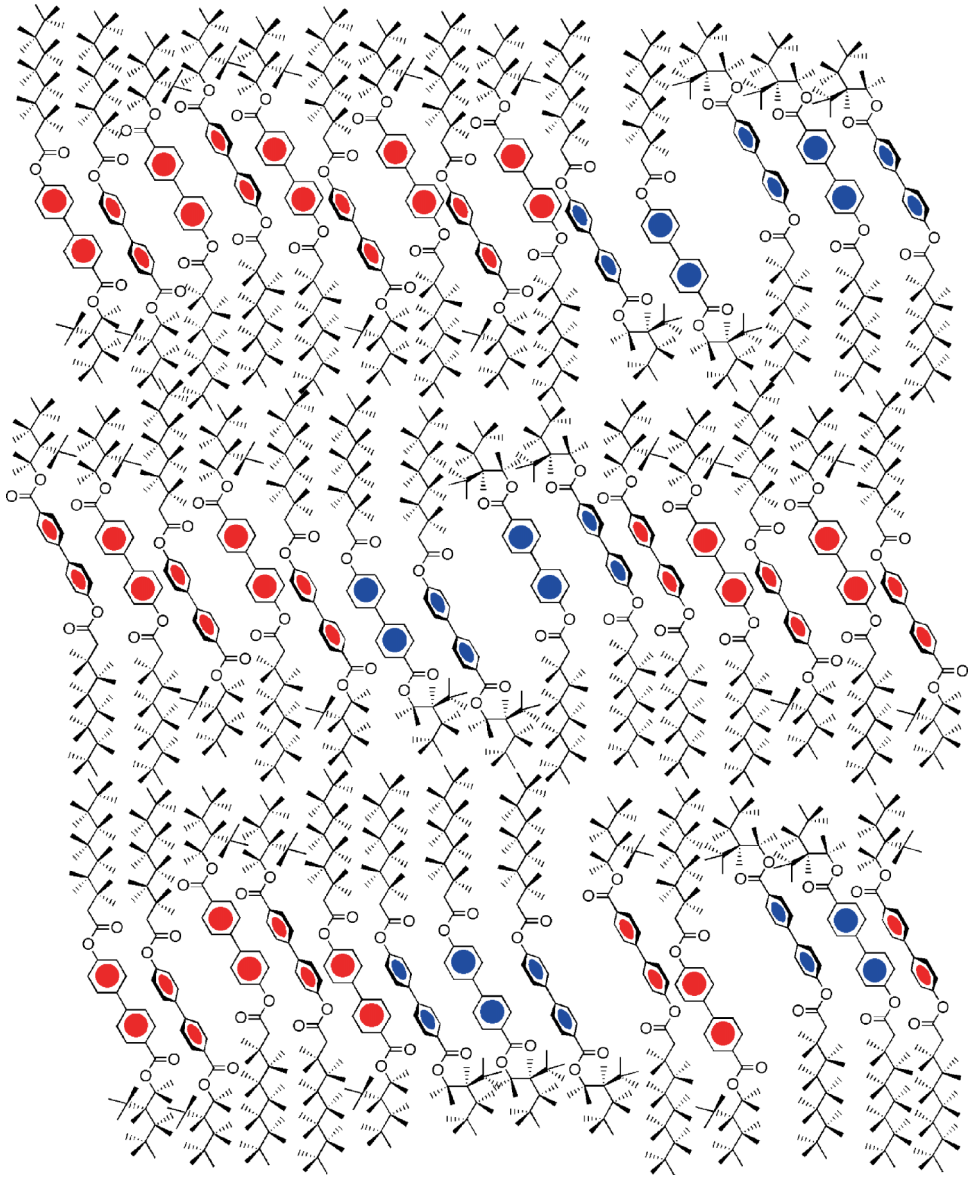

Figure 36. An ensemble of two conformational species *A* and *B* in a dynamically fluctuating smectic C phase.

Figure 37. Materials that exhibit helix inversion as a function of temperature in the chiral nematic phase.

positions of their aliphatic chains. For calamitic systems, this class of materials is overly represented by reactive mesogens where the two terminal groups are photopolymerisable units such as acrylates, methacrylates, oxetanes, dienes, etc. (*76*, *77*).

Three examples of reactive mesogens are shown in Figure 38. In keeping with the previous discussions, these are derivatives of difluoroterphenyls that can be compared with similar materials possessing straight aliphatic chains. The first two compounds, which are

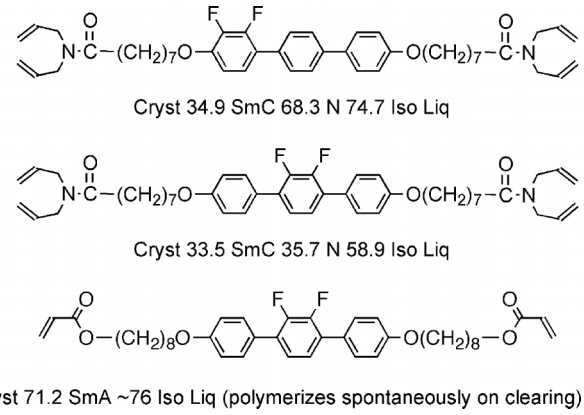

Figure 38. Reactive mesogens that carry two terminal functional groups designed to undergo photopolymerisation.

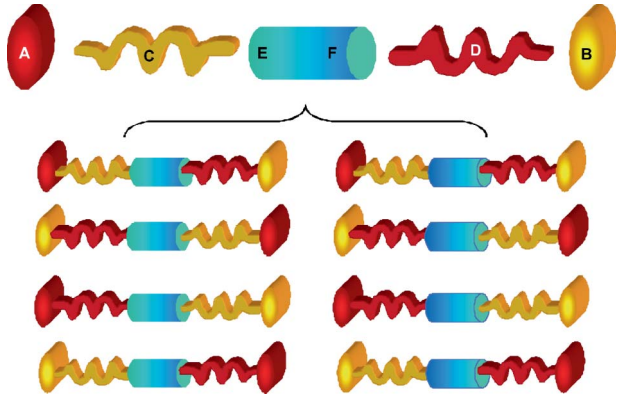

Figure 39. Variations for potential structures of materials possessing two terminal functional groups in the flexible chains.

derivatives of diallylamine (*78*) exhibit similar phase sequences to the parent systems, with nematic and smectic C phases being found. It is important to note in these cases that the melting points are very low. Conversely, the acrylate derivative has a high melting point and was only found to exhibit a smectic A phase, with no nematic or smectic C phase being present (*24*, *79*). Consequently, even for reactive mesogens, the nature, size, shape and polarity of the terminal functional group affects the mesophase type and properties. For photopolymerisations in the liquid-crystalline state the structure of the mesophase may be controlled by the terminal photopolymerising group, and hence this can be used to determine the properties of the ensuing polymerisation product (*78*). Thus, for the diallylamine derivatives shown in Figure 38, polymerisation can take place in the nematic, smectic A and smectic C phases, whereas the polymerisation for the acrylate can only take place in the smectic A phase.

By the very nature of their synthesis, reactive mesogens typically possess symmetrical structures with respect to their terminal functional groups, and there are very few materials that possess differing end groups. However, for systems with differing end groups the complexity increases quite considerably. For materials having methylene spacers attaching the terminal groups to an asymmetric core, there are eight possible configurations for a potential molecular architecture, as shown in Figure 39. The number of possibilities can be even larger if the linking unit between the terminal moiety and the core has directionality, i.e. one end of the linking unit (C and D in Figure 39) is different from the other. A similar conclusion can be drawn from having terminal groups that also have directionality and so too can be inverted.

6. Supermolecular strings: bimesogens, dimesogens, trimesogens and tetramesogens

The first step in creating linear supermolecular materials, or molecular strings, is to extend molecular design to the creation of superstructures possessing more than one mesogen. The simplest architecture is a system possessing two identical mesogens, described here as being bimesogens. The next step up in complexity is to have two non-identical mesogens, termed dimesogens. Beyond two mesogenic units being tied to one another, liner systems possessing three units or more must have some different mesogenic units. For example a trimer could have two identical mesogenic units at the ends of the linear structure, i.e. in positions 1 and 3, but the centre mesogen will necessarily have a different structure simply because it is tied to two mesogens whereas the terminal mesogens are only tied to one. Thus, the dynamics of the centre mesogen will be different to the exterior mesogens in the linear chain.

Generally for all linear architectures where the aromatic mesogenic cores are linked by aliphatic chains, the homologues that have connecting spacer chains with an even number of methylene units have much higher clearing points in comparison with the systems with an odd number of methylene units. This is because the odd members tend to have bent conformational structures which induce disordering into the mesophase structure, whereas the even members tend to have linear *trans* structures which support mesophase formation (*80*, *81*).

6.1 *Bimesogens*

Following on from the work that described monomeric terphenyls, Figure 40 shows some examples of difluoroterphenyl bimesogens where the liquid crystal

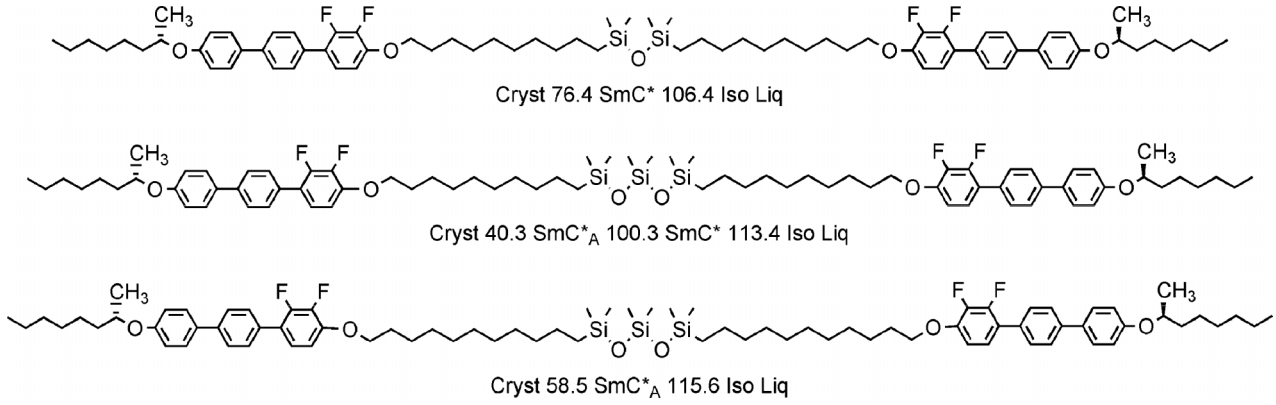

Figure 40. Bimesogenic supermolecular liquid crystals with silyloxy bridging units (*84*).

units are identical (*82*). In each example, the mesogenic moieties are joined together via methylene chains and a linking siloxane bridging unit. The incorporation of such bridging groups can affect the overall packing of the molecules leading to reductions in melting points and the stabilisation of lamellar smectic phases over nematic phases. In the three examples shown, the combination of the two linking methylene chains and the siloxy bridging group is of such a length so as to favour the formation of lamellar phases at the expense of the nematic phase. As the mesogenic units are chiral in these materials, the lamellar phases too are chiral. Orthogonal phases are also suppressed and, as is the case for many bimesogens, no higher ordered smectic phases are observed. Thus, although the molecular architecture has increased in complexity, the complexity associated with the liquid crystallinity has decreased. The length and nature of the combined spacer unit is noted to have the effect of favouring synclinic over anticlinic structures, or *vice versa*. For the materials shown in Figure 40 synclinic properties give way to anticlinic properties as the length of the bridging unit is increased in length along with the methylene spacer. Thus, too, the materials change over from being ferroelectric to antiferroelectric.

6.2 Linear dimesogens, trimesogens and tetramesogens and non-mesogenic systems

Moving to dimesogens, as opposed to bimesogens, the complexity of the molecular architecture increases eightfold, as shown in Figure 41. Now it matters which way round the mesogens are attached to the spacer unit, and indeed if the spacer unit itself is asymmetric; as such, the way round it is incorporated into the architecture also matters.

Dimesogens, trimesogens and tetramesogens, etc., can have very subtle differences in structure. For example, the dimesogen shown in Figure 42 has two

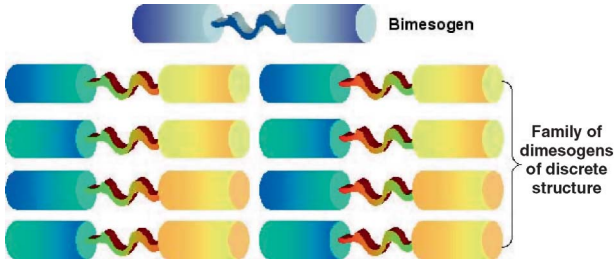

Figure 41. Complex architectures for dimesogens in comparison with bimesogens.

different mesogenic units, i.e. a steroidal moiety and a Schiff's base unit, where one is chiral and the other is not (*83*). The properties of this material are roughly averaged between the two mesogenic groups.

The trimesogen shown conversely has similar mesogenic units all based on the biphenylyl motif, thus there is a central biphenylyl unit with two external cyanobiphenyl units attached to it (*84*). Although the aromatic mesogenic moieties are structurally similar, the polar, and thereby strongly polarised, cyanobiphenyl units will impart very different properties in comparison to the central biphenylyl entity.

The tetramesogen (*85*) in Figure 42 has four identical aromatic units based on the phenyl benzoate motif. However, the external two units possess exterior flexible aliphatic chains, whereas the interior two units have linking aliphatic chains that are tethered to aromatic systems, and therefore these two mesogenic units will have different mobilities and, hence, properties in comparison with the exterior aromatic mesogenic groups. Moreover, the differences in mobility and, hence, molecular dynamics associated with the rigid aromatic units of the dimesogenic, trimesogenic and tetramesogenic systems means that these systems will also have different interactions and, hence, properties relative to simple mesogenic systems with architectures composed of two aliphatic chains and one inflexible core unit.

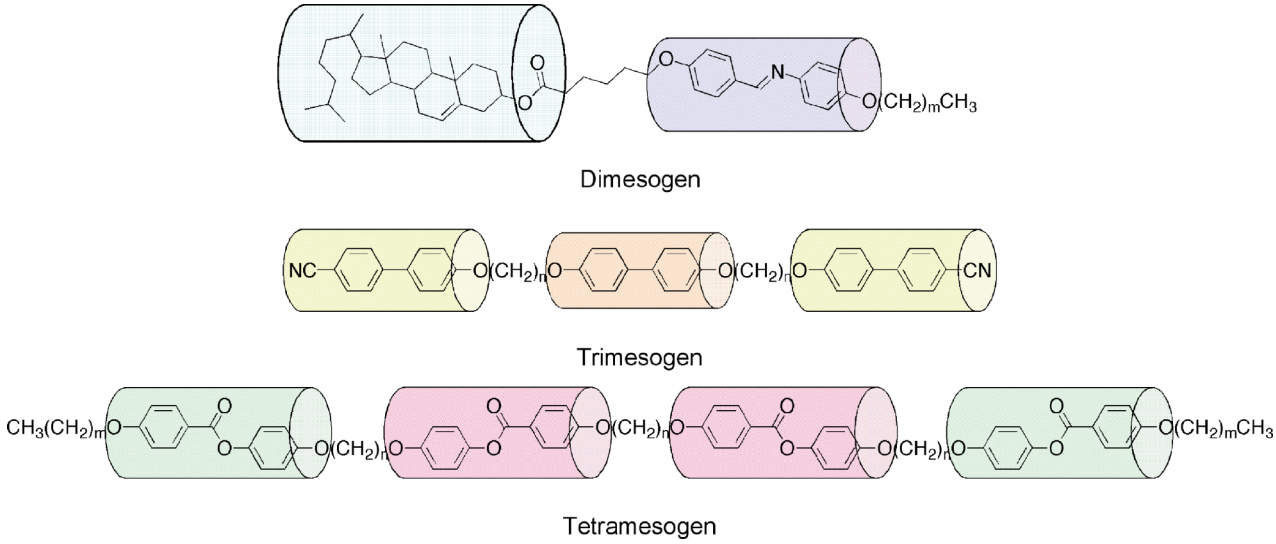

Figure 42. Examples of typical dimesogenic, trimesogenic and tetramesogenic liquid crystals.

This general picture, and its consequences, is exemplified through a number of systematic studies by Nishiyama *et al.* into dimeric and trimeric liquid crystals (*86–97*). Investigations were made first on deploying the same mesogens in dimeric systems but with accompanying variation of the linking group, and secondly on incorporating non-mesogenic units into supermolecular architectures, but with the result that mesomorphic materials were still obtained.

The first set of four materials, shown in Figure 43, all possessed the benzoyloxy-biphenylyl unit commonly deployed to support the formation of antiferroelectric properties in liquid crystal systems. All of the materials were designed to be chiral via the incorporation of 2-octyl moieties with both *RR* and *SS* variants being available for the resulting bimesogens. With a simple alkyl-linking unit between the mesogens, a phase sequence of ferroelectric–ferrielectric–antiferroelectric as a function of temperature was found (*88*, *89*). When the linking group was changed to a di-thioether (*95*) unit, ferroelectric and ferrielectric properties were suppressed in favour of antiferroelectric phase

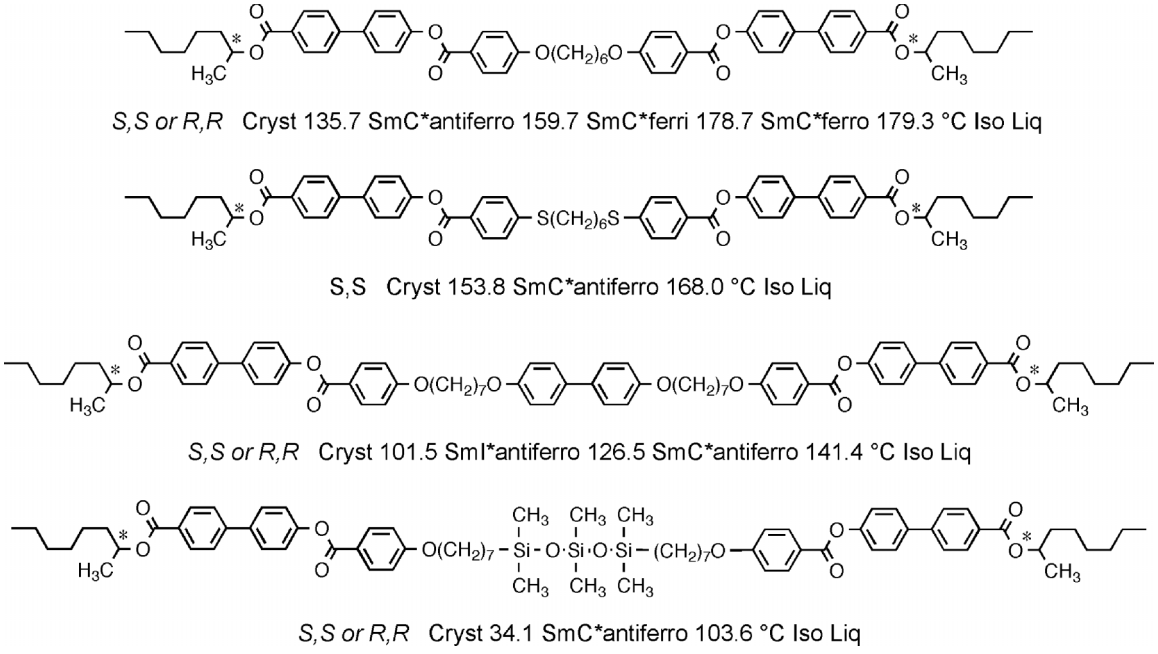

Figure 43. A systematic study of the change in linking groups in dimeric and trimeric liquid crystals.

formation, see the second structure. It is known from other investigations that the incorporation of sulphur in place of oxygen in aliphatic chains tends to favour the formation of more ordered phases such as the crystal B phase over the hexatic smectic B phase (*98*, *99*).

Through the incorporation of a biphenylyl unit in the bridging chain in order to create a trimesogen, higher-ordered antiferroelectric phases, such as the smectic I^*_A phase, were found, see the third compound in Figure 43 (see also (*97*)). Lastly for this family of materials, the linking group was substituted with a siloxy unit (*93*). Siloxy substitution has the effect of lowering melting point and, for an odd number of atoms substituted into an even number of atoms in the methylene chain, antiferroelectric phases are stabilised. For the last compound, this is the case with a melting point of only 34.1°C and the other supermolecular materials having melting points above 101.5°C. As the number of atoms located in the chain between the two mesogenic units is odd, the overall structure is bent, and therefore antiferroelectric phases are stabilised.

Interestingly, additional studies by Nishiyama *et al*. (*86–97*) demonstrated that when, taken in isolation, only one of the aromatic units within a supermolecular system has a propensity to exhibit liquid crystal phases, then the supermolecular material itself could be mesomorphic, see Figure 44. For example, for the top molecular structure (*97*) only the biphenyl unit at the centre of the structure supports mesophase formation, whereas the benzoate units are too isolated from the biphenyl moiety in order to affect mesomorphic behaviour. The second material (*97*) has terminal phenyl units, which are only connected by aliphatic chains to the benzoate units. Thus, in this case the material has four aromatic units out of six which are not in positions that can enhance mesophase formation. However, the second material has similar transition temperatures and phase sequences to the first, i.e. both materials exhibit an unidentified smectic phase and a synclinic ferroelectric smectic C* phase. If the third material is examined, it can be seen that the mesogenic unit at the centre of the supermolecule is an azobenzene unit which is typically more strongly supportive of mesophase behaviour than the simple biphenyl moiety (*90*). The attachment of the terminal phenyl unit is by a methylene spacer of odd parity, and as a consequence the smectic C phase has an anticlinic structure rather than synclinic. It is interesting, however, that the three materials surprisingly have similar melting and clearing points considering that they have quite different structures. It is as if the overall supermolecular structure, consisting of three mesogenic sub-units, should be considered as an extended rod-like architecture where the local interactions along the rod are less important than the overall shape. Thus, the complexity is effectively being reduced.

These studies demonstrate that for supermolecular materials it is not necessary to have all of the aromatic/rigid units being supportive of mesophase formation for a supermolecular material to be mesomorphic. Odd parity spacer units tend to support anticlinic properties, whereas even parity spacers support synclinic properties.

6.3 *Supermolecular strings: multiple mesogenic units*

If we take this architectural description further for liquid crystals with multiple mesogenic units, i.e. mesogenic strings, where the mesogenic units are of clearly different structures, then the complexity increases almost exponentially. For example, if we take just a simple mesogen with two flexible asymmetric but

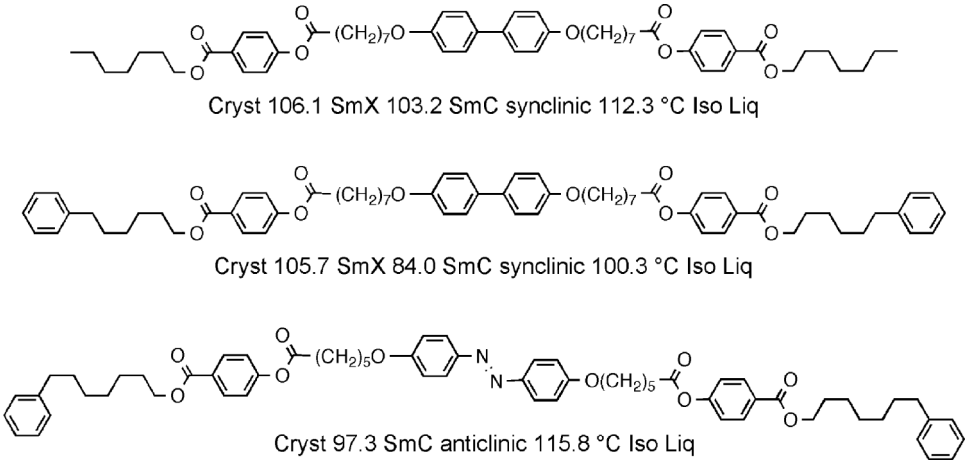

Figure 44. Supermolecular liquid-crystalline materials consisting of only one unit that has mesogenic tendencies.

different peripheral chains and an asymmetric inflexible central unit the combinations for the structural arrangements of these three segments is 8 (see Figure 2). For a bimesogen this number increases to 16, but for a dimesogen it is even greater at 128. Thus, for multiply segmented mesogens with n segments arranged in any order in a linear supermolecular architecture of m mesogens in any order, the number of structural components is $4n!m!$.

The complexity found in linear supermolecular liquid crystals is exemplified by the general structure for the tetramesogen shown in Figure 45. Assuming that the mesogens possess three segments with a non-flexible unit at their centres, the number of possible structural variations for this architecture is in excess of 1.5 million. Moreover, when linked together it is also not apparent where one mesogen ends and another starts. Thus, the mesomorphic properties become smeared out because of the lack of definition in the structure and, hence, the molecular interactions become ill-defined. As a consequence, ordered mesophases, anisotropic plastic crystal phases, etc., are less likely to occur.

6.4 Supermolecular knots: trimesogens, tetramesogens and octamesogens with a focal point

Trimesogens are the first supermolecular systems that can be designed not to have a linear structure, instead they can have a structure that has a focal point: a molecular knot rather than a string. Following on from the examples of monomeric and dimeric difluoroterphenyls, trimeric systems for which comparisons can be made may only be achieved by having all three difluoroterphenyl mesomeric units in the same environments, i.e. by tying them together at one focal point, unlike a linear system which as noted earlier must invariably have at least one mesogenic unit different to the other two.

Figure 46 shows an example of a trimesogen where the difluoroterphenyl units are bound to a central siloxane scaffold (*82*). In addition, the results for the trimer are compared with the linear dimer in the same figure. Both the trimer and dimer exhibit the same liquid crystal phase, which is anticlinic and because the materials are chiral the phase is also antiferroelectric. Both dimer and trimer have bent architectures owing to the odd number of atoms in the linking chains between the mesogenic core units. The bent supermolecules can pack together in an alternating intercalated way so as to create a layered anticlinic mesophase. Interestingly, the melting points are within 10°C of one another, and the clearing points within 20°C. In terms of the mesomorphic behaviour of these two materials, the transition temperatures and phase sequences indicate there is little difference between the two. Thus, although the bimesogen can be considered to have a linear structure, whereas the trimesogen is a molecular knot, they essentially have very similar molecular architectures, i.e. the bimesogen has a bent structure because of the odd number of atoms in the linking and bridging chain uniting the terphenyl cores, the trimer, similarly has a bent structure as shown by the diagram in the centre of Figure 46. The interesting result is that the anticlinic liquid crystal mesophase can support both of these molecular architectures in an intercalated organisation (shown by the different coloured mesogens in the figure) such that the number of mesogenic units in the supermolecular structure does not matter.

If we now consider a tetramer, see Figure 47, of similar structure to the dimer and trimer (*82*), the addition of the extra mesogenic unit should have the effect of producing an overall molecular shape that is tubular. Thus, it should be more unlikely that this material will exhibit a synclinic mesophase over an anticlinic organisation. Interestingly, the melting point is lower than either the dimer or trimer; however, the clearing point is very similar. The similarity of the clearing points suggests that the number of mesogenic units in the supermolecular structure, and hence the associated dispersion, is almost irrelevant with respect to mesophase stability. Thus, the local intermolecular interactions are less important than they are for simple monomeric systems, and therefore molecular shape is starting to become the dominant factor in phase formation. This is further exemplified by the potential separation and packing of the siloxy units together to give a multi-stacked organisation as shown in Figure 48.

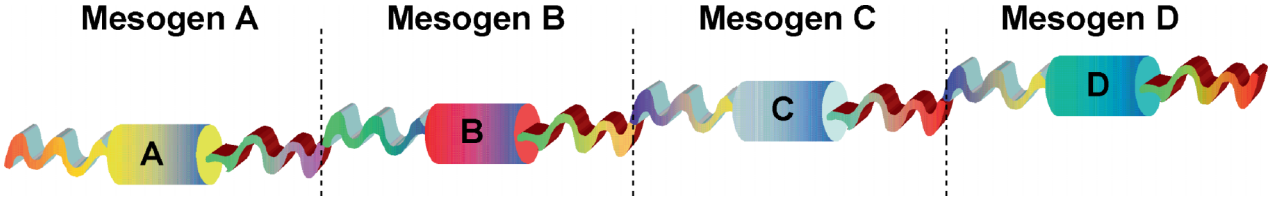

Figure 45. A diagram representing one structure out of over 1.5 million possible structures for a linear tetramesogen.

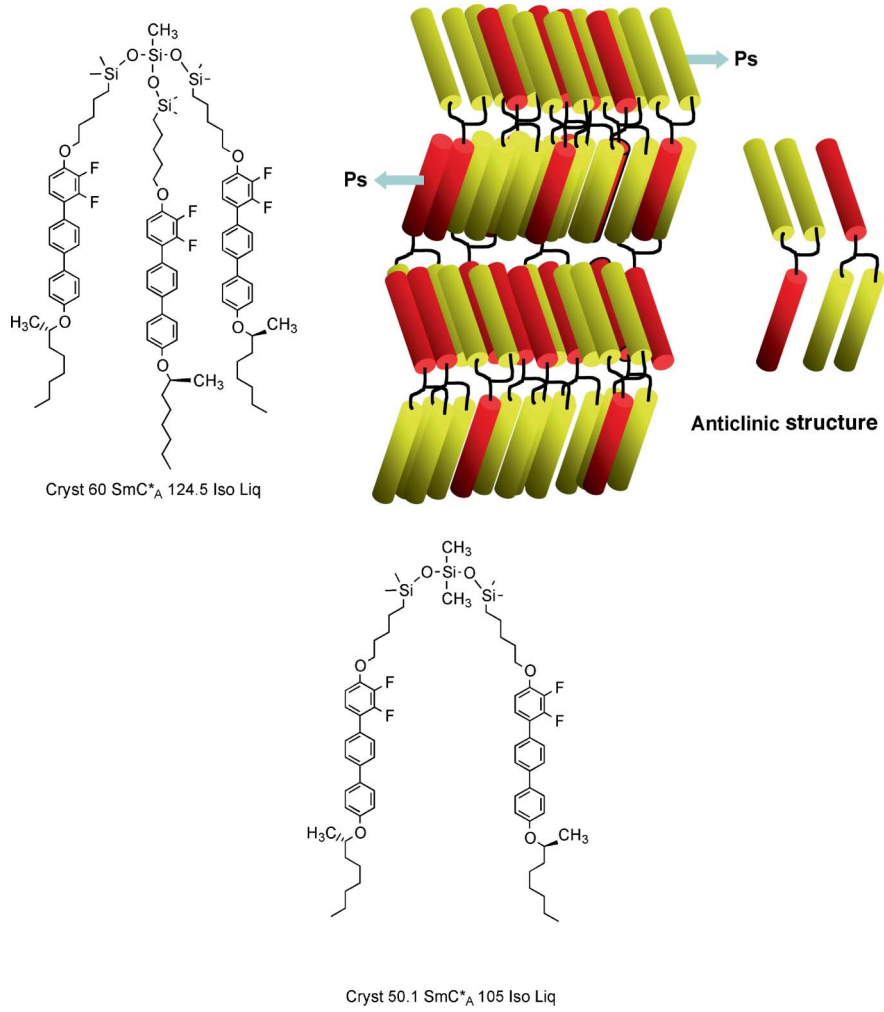

Figure 46. Comparison of a dimeric and trimeric difluoroterphenyl based supermolecular liquid crystals. Both materials exhibit anticlinic and antiferroelectric liquid crystal phases, as shown by the diagram in the centre of the figure for the trimesogen. In this cartoon, the mesogens are coloured differently to clarify the structuring to show that the layers can be intercalated.

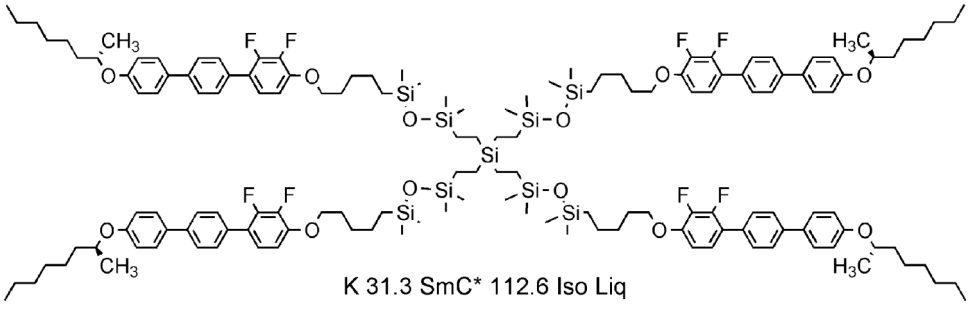

Figure 47. A supermolecular tetramer.

Examination of the mesophase structure exhibited by the tetramer shows that it forms a tilted phase, with the tilt angle growing as a function of the reduced temperature. The results were consistent with the phase being smectic C and therefore synclinic. Electrical field studies, on the other hand, showed that the tetramer may exhibit antiferroelectric behaviour, and therefore the tilted phase is anticlinic. Modelling shows that both structures are possible, and there is little advantage of one organisation over the other, as

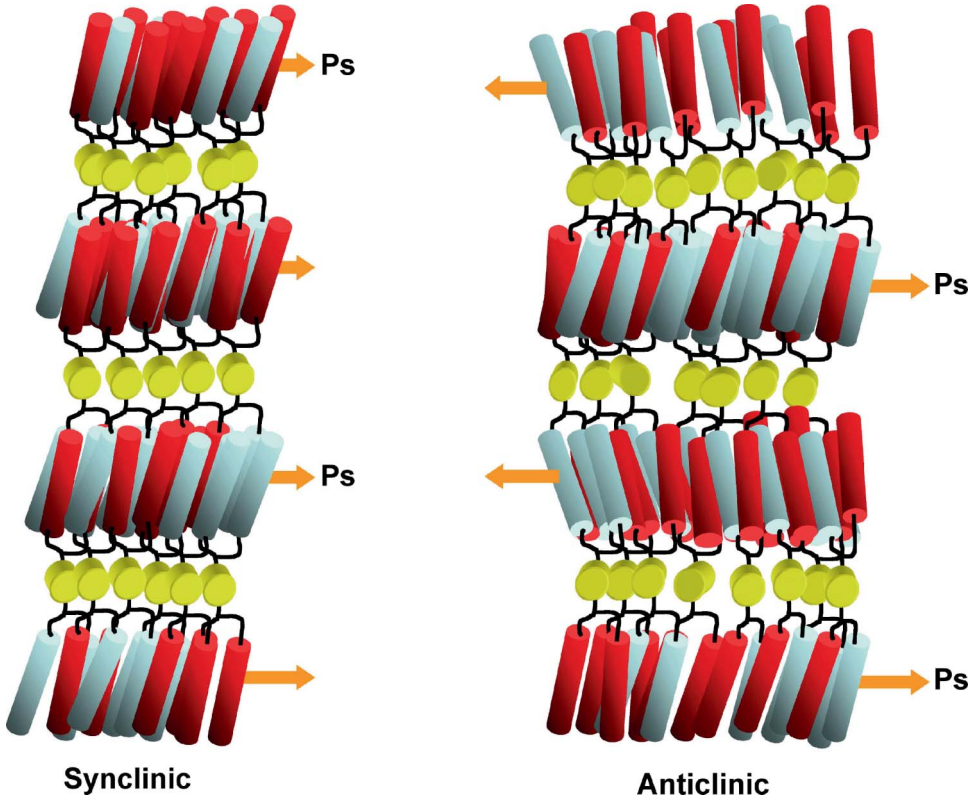

Figure 48. Comparison of the synclinic and anticlinic structures of the supermolecular tetramer.

shown in Figure 48. Thus, the tetramer is probably sitting at the point where there is a change from anticlinic to synclinic behaviour. Consequently, in Figure 48 the mesophase formed is stated as smectic C, but its clinicity is not defined.

With the supermolecular architectures described in this section it is difficult to continue adding more mesogens to the central scaffold in order to examine how the overall molecular shape changes, and thereby affects mesophase structure. However, by adding more mesogens to the structure it is expected that the molecular shape would become cylindrical, and therefore the smectic A phase would start to dominate. This is similar to the behaviour exhibited by monomeric materials, as shown in Figure 15, where cylindrical structures are depicted to disfavour ordered and/or tilted mesophases.

These predictions can be explored in part by examining the properties of the difluoroterphenyl octamer based on the octasilsesquioxane scaffold, as shown in Figure 49 (see also (*82*)). This material

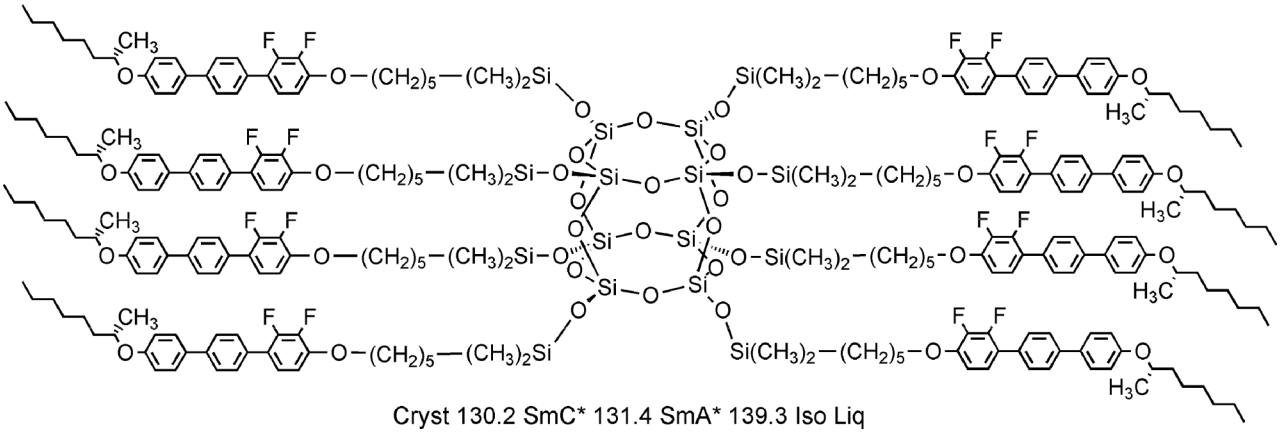

Figure 49. An octamer of difluoroterphenyls based on an octasilsesquioxane scaffold.

exhibits smectic C* and smectic A* phases, and its clearing point is only 139.3°C, which is only marginally higher than the trimer. The transition to the smectic C* phase is 131.4 °C, which is approximately 7°C higher than the trimer, conversely the melting point in comparison is high at 130.2°C which reflects the symmetrical nature of the molecular architecture. The formation of the smectic A* phase is due to the fact that the molecular shape is tubular rather than bent, and as a consequence a synclic phase occurs at a lower temperature rather than an anticlinic phase. As with the tetramer described previously, the organisation of the layers of the octamer will be in slabs of aliphatic chains, aromatic cores and octasilsesquioxane scaffolds as shown for the local structure of the synclinic smectic C* phase in Figure 50.

Thus the results for the dimer, trimer, tetramer and octamer reflect a mass/molar dependency with respect to the physical properties. The interactions between the mesogenic groups may be additive, but they also will be a function of the number of mesogens in the supermolecular structure, hence the upper transition temperatures for the four supermolecules are roughly the same. Moreover, this result also indicates that the mesogens dominate the self-organisation process, and the slight variations in transition temperatures are due to differences in the scaffold structure. Furthermore, the nature of the smectic C phase, synclinic or anticlinic, is dominated by molecular shape rather than by the mesogenic interactions, unlike the situation for simple monomeric species.

So here we are at the point where the local interactions, shape, polarity, stereochemistry, conformation and 'microphase segregation' that determine mesophase formation on the nanoscale give way to mesophase formation being dominated by shape in the mesoscale regime. As a consequence, it should be expected that smectic polymorphism associated with nanostructuring will be suppressed and that shape-dependent mesophases, lamellar, hexagonal and cubic will dominate the mesoscale structures. As such the shape dependency will be linked to the number/density of mesogens attached to the scaffold, as shown in Figure 51. Thus, as the molecular structures of supermolecules become greater, and the outward structure becomes more complex, the mesophase properties actually become simpler.

At this level of complexity, as shape appears to be the predominant factor in determining the self-organising process, the structures of the supermolecular systems could be simplified. For example, the mesogenic groups could be omitted leaving the

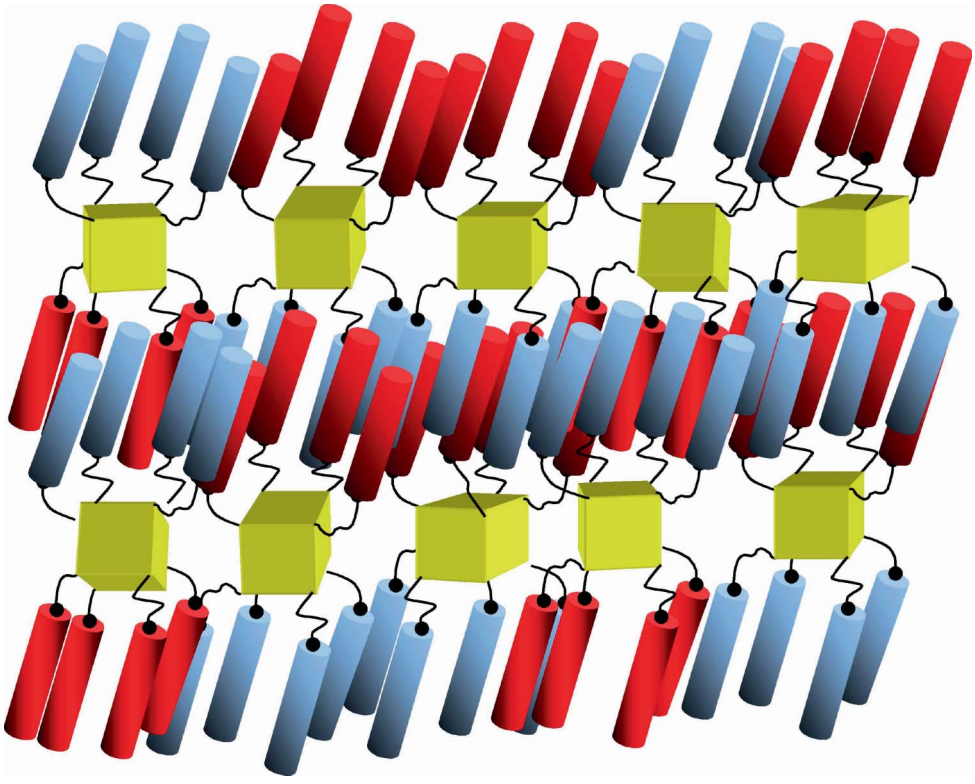

Figure 50. The synclinic structure of the supermolecular octasilsesquioxane octamer showing segregation between the aromatic mesogens and the silsesquioxane scaffolds.

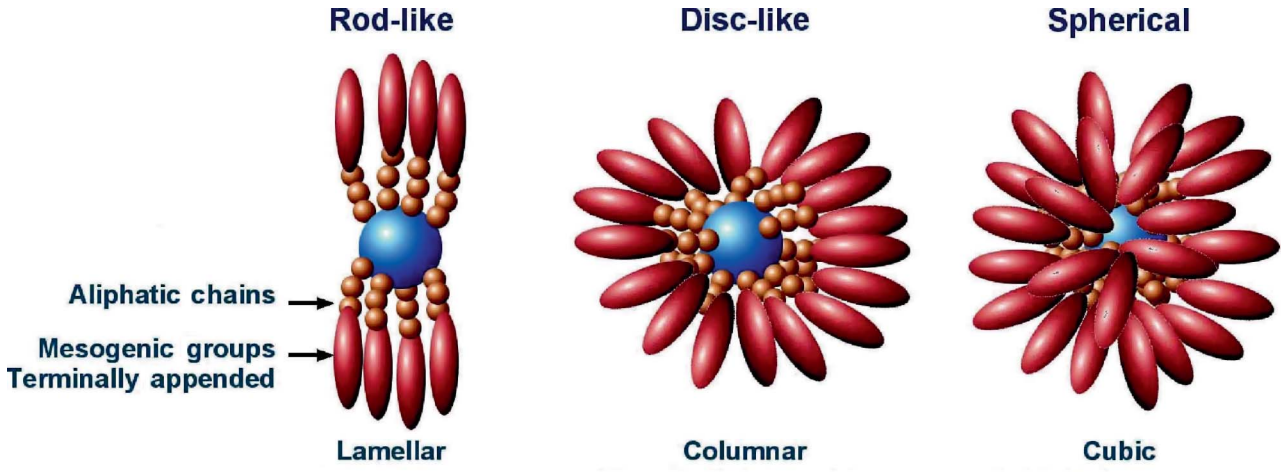

Figure 51. As the number of mesogenic units attached to a central scaffold is increased, the overall shape of the resulting supermolecule changes from being rod-like to being spherical. The shape change results in a progressive change in associated phase type from lamellar to cubic via columnar.

scaffold coated with just aliphatic chains, as shown in Figure 52 (see also (*100*, *101*)). Again the density of the chains attached to the scaffold is all-important in determining shape, thus bifurcation of the chains can be a useful design feature for creating such systems. Often bifurcation has been achieved using a 1,3,5- or 1,3,4-trisubstituted phenyl ring as the bifurcation point (*100*, *102–104*). This construction leads to a better two-dimensional spacing of the chains through the flat aromatic ring. The result is a simple molecular architecture of a fatty rod, a fatty disc or a fatty sphere, that would not be recognised as any structure that would support conventional liquid crystal mesophases.

6.5 *Chiral nano- and meso-objects*

If shape is the determinant for the self-organisation of supermolecular systems, then obviously surface topography is an important issue to consider for rods, discs and spheres, and combinations thereof. For example, we could have a situation for rod-like supermolecular architecture where the surface of a scaffold that is rod-like is coated through lateral attachments with rod-

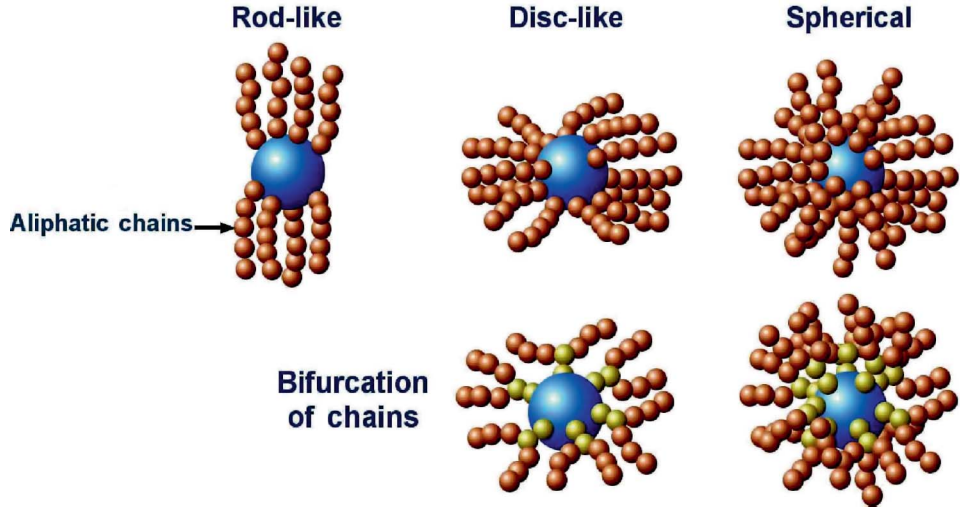

Figure 52. The shapes of supermolecular systems can determine mesophase formation even if the supermolecular system possesses no mesogenic groups. In this figure the density of aliphatic chains on the surface of a central scaffold is used to produce rod-like, disc-like and spherical supermolecules which can support lamellar, columnar and cubic mesophase formation, respectively. Bifurcation in the exterior chains can induce curvature in the shapes of the supermolecules at a lower density of attachments to the scaffold, as shown in the lower part of the figure.

like mesogenic constructions. When the lengths of the mesogenic rods are slightly longer than the comparable width of the scaffold, but the density of mesogens on the surface is relatively low, the mesogens will form roughly parallel arrangements, such as a nematic phase; however, the scaffold may pack in a different arrangement, for example hexagonal. Thus, it is possible that new 'combination' mesophases will occur based on lattices created by the competition between the packing of the scaffolds and the attached mesogens. Thus, for rod-like mesogens attached to a rod-like scaffold the result may be a 'tubular-nematic' columnar phase, as shown in Figure 53.

If the number density of the mesogens is relatively high and their lengths substantially longer than the dimensions of the scaffold, then chiral structures can be formed due to the inability of the mesogenic rods to pack flatly on the surface of the scaffold. The rods will organise themselves to be parallel but because they are too long they will twist away from the long axis of the scaffold, which can result in their spiralling about the scaffold, see Figure 54. Similar results have already been found for rod-like mesogens attached to a cubic scaffold (*105*). In this situation both left- and right-hand spiralling structures associated with a helical director field about the rod-like scaffold may be obtained. Where the rod-like mesogenic units are themselves chiral one helical structure will dominate, which will lead to a molecular line defect down the centre of the cylindrical scaffold, almost like the twist cylinders associated with Blue Phase defect lines.

For a combination of a spherical/cubic scaffold, such as octasilsesquioxane and rod-like mesogens laterally attached to the surface of the scaffold by aliphatic spacers, a spiralling director field about the sphere similarly could be obtained. However, in this case, because of the spherical scaffold, the director field

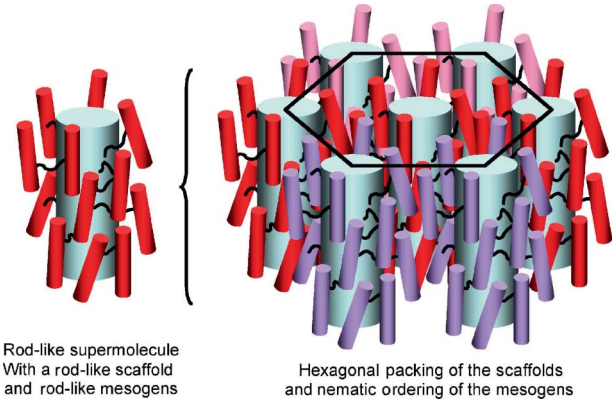

Figure 53. Combination 'tubular-nematic' hexagonal columnar mesophase formed by the packing of rod-like mesogens on the surface of a rod-like scaffold.

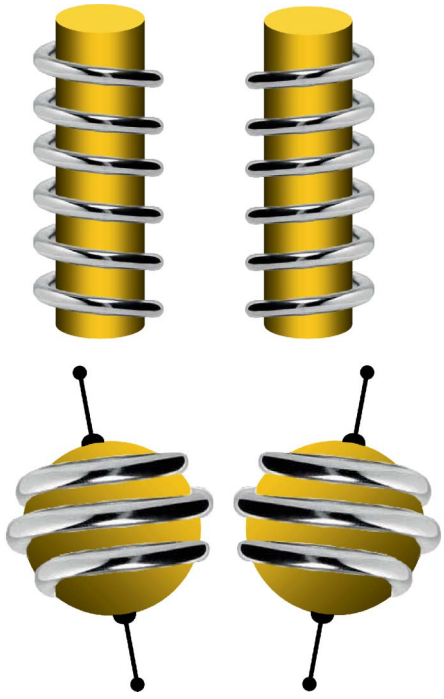

Figure 54. Spiralling nematic director fields shown in silver for a gold-coloured surfaces of central scaffolds of supermolecular liquid crystals. The spherical scaffold possesses defects centred at the poles, whereas for the cylinders there is a line defect down the centre of the cylindrical scaffold.

would create defects at poles on the surface of the sphere, i.e. a *'molecular boojum'* could be created as shown in Figure 54 (see also (*106*)). Thus, the nanostructured supermolecular material would have a chiral surface which would affect in turn its abilities as a *'chiral object'* to self-organise.

An example of a supermolecule possessing a spherical scaffold with chiral mesogenic units laterally linked to the scaffold is shown in Figure 55 (*106*). The lengths of the rod-like mesogens are of a similar size to the diameter of the scaffold which is composed of a [C_{60}] fullerene with short aliphatic linking units. The mesogenic units are chiral by virtue of having asymmetric terminal aliphatic chains derived from (*S*)-2-butanol. The linking units are bifurcated, thereby allowing 12 mesogenic units to surround the spherical core of the scaffold. Modelling demonstrates that the mesogens cannot pack together around the fullero-scaffold without twisting. As they are chiral the twist will be in one preferred direction, hence a '*molecular boojum*' is potentially formed with defects at the poles. The material itself, because the mesogens are laterally attached, exhibits a chiral nematic phase from the glass at 47°C to the clearing point at 103°C.

Figure 56 shows a schematic representation of the fullerodendrimer with the mesogenic units spiralling

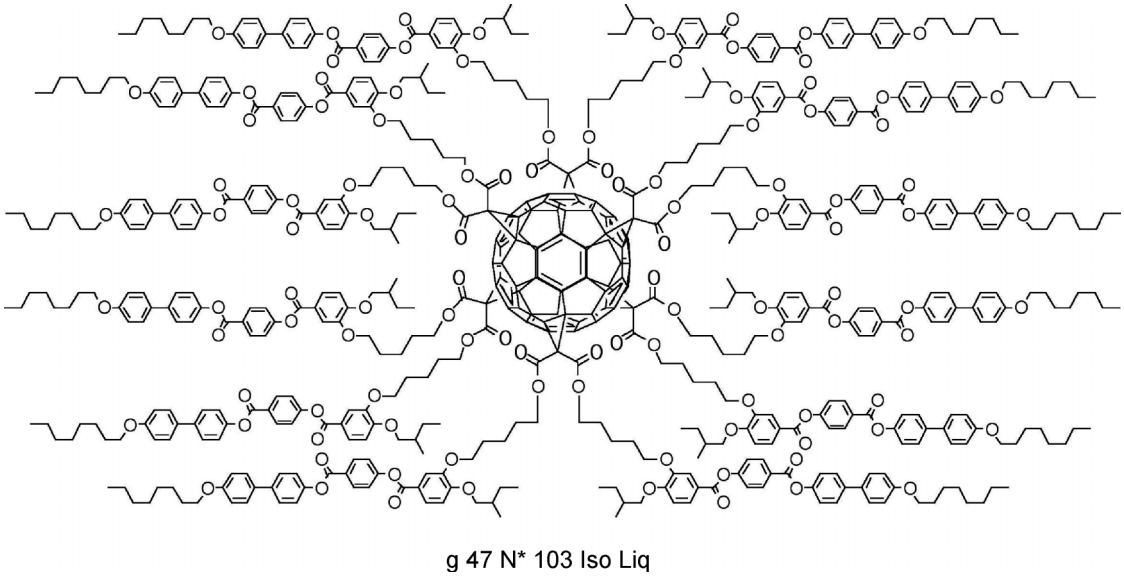

Figure 55. A chiral fullerodendrimer which exhibits a chiral nematic phase.

around the spherical scaffold. Such spherical nanostructures that possess a helical surface topological relief can pack together through their defects so that the twist might propagate, and/or by packing twisted structures together to create cubic phases with similar structures to those of Blue Phases. Although this is a relatively small-scale system, if the scaffolds are increased in size, this may be via the use of a nanoparticle at the centre, such as gold, the surface decoration by laterally appended chiral mesogens can also create spheres with topological reliefs. Thus, extremely large-scale lattices may be possible with quasi-bonding between the particles.

Other possible defect structures associated with nematic director fields confined in spherical geometries have been envisaged by Nelson and co-workers (*107–109*) and Bates (*110*, *111*). For example, nanoparticles with laterally appended mesogens could have surface defect structures, with four singularities being a preferred option, see Figure 57. Packing of such nano-structured supermolecular systems may be through lattices of defects, and in the case of the sphere shown in the figure this would create a tetrahedral arrangement of defects and hence a tetrahedral lattice of the spheres. Thus, we have reached the point of large molecular systems, by virtue of their shapes, topography and locations of their defects, where they can potentially form large-scale lattices giving quasi-crystalline order as shown in the right-hand part of Figure 57 which depicts a diamond lattice.

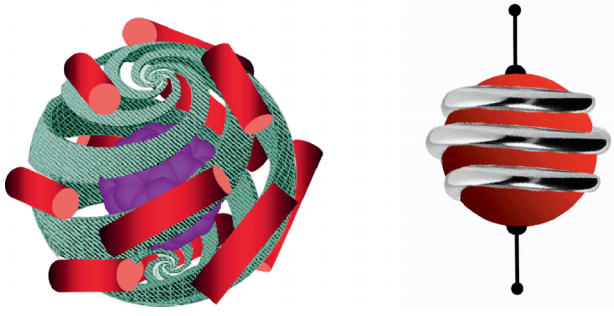

Figure 56. Schematic representations of the chiral nanoparticle.

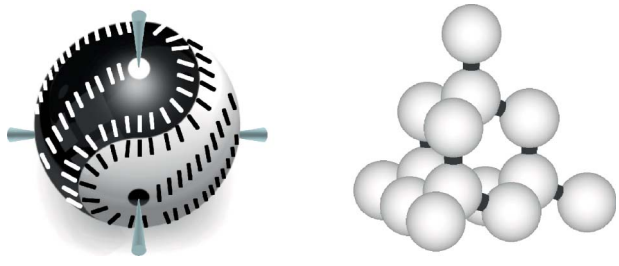

Figure 57. An example of a nematic director field confined in a spherical geometry where there are four defects arranged in a tetrahedral configuration, and an organised structure created through packing along the defect lines.

7. Functional and multipedal supermolecules

For the dendritic materials described above the mesogenic entities attached to the central scaffold have all been the same. The results show that the higher the density of mesogens coating the surface of the scaffold, the less relevant the dispersity of the system. Thus, such materials are architecturally of low complexity. However, in Section 6.3 linear supermolecules made up of chains of mesogens were discussed. In ending this study it is interesting to revisit this concept, but this time with differing mesogenic (or non-mesogenic) moieties attached to the central scaffold thereby creating a multipedal system, see Figure 58. In the earlier analysis, the number of architectural variations for a tetramer was shown to be in excess of one million; however, for a tetramer with a tetrahedral scaffold the number of variations is 2×8^4, which is considerably less. Thus, molecular knots are much less complex than molecular strings.

Typically, however, the tendency is to have, say for example, three units the same, with one being different, or two pairs the same and different to the other pair (*112*, *113*). Obviously for larger systems the possibilities are greater, and have led to examples of supermolecular materials composed of two different halves or faces, the so-called 'Janus liquid crystals' (*114*, *115*).

One example of a functional supermolecule possessing difluoroterphenyl mesogenic groups has been reported as exhibiting the much sought after biaxial nematic phase (*116–118*). This material, shown in Figure 59, comprises three rod-like units and one disc-like moiety. The rod-like mesogens impose a positive birefringence, whereas the disc-like moiety provides a negative birefringence, with the material exhibiting properties of both resulting in it supposedly being biaxial. The higher degree of complexity in relation to the molecular architecture results in such systems exhibiting smectic polymorphism, in this case nematic, smectic A and smectic C.

When this material is cooled from the isotropic liquid it first forms a nematic phase. The disc-like moieties favour the nematic phase over columnar phases, whereas the difluoroterphenyl units classically support nematic, smectic A and smectic C phases. Thus, it is interesting that this phase sequence is obtained on cooling. The nematic phase, however, is relatively thermodynamically stable, possibly because the disc-like units suppress layer formation. It is possible that the packing of the supermolecules together prevents the rotational disordering of the discs by the rods, as shown in Figure 60. Locally, therefore, the mesophase is biaxial, but over longer distances it might indeed approximate to being uniaxial.

8. Summary

In summary, we have used this conceptual article to describe how the availability of intermolecular interactions influence mesophase formation and stability at the nanoscale length regime. We describe how the whole of the molecular architecture and its interactions have to be considered and as a consequence the longitudinal interactions are equally as important as the lateral interactions that are usually manipulated in the process of the molecular design of materials of commercial interest. Thus, taking a 'holistic' approach, we conclude that it is the strength of the allowable dipolar and quadrupolar interactions which are dependent on the dynamic and static steric shapes of the molecules that determine mesophase stability.

Upscaling of molecular structure to the meso-length scale appears to result in the smearing out of the intermolecular interactions, and as a consequence molecular shape becomes the important determinant of mesophase formation. At such length scales, therefore, it is less likely that polymorphism will be observed, and thus the mesophases will fall into the three classes of lamellar, columnar and cubic. Moreover, it appears that molecular topology and surface relief in nano-objects can result in molecular defects which may affect the organisation of supermolecular structures over reasonably long length scales.

Acknowledgements

We would like to thank the Leverhulme Trust, the Department of Trade and Industry, the Royal Society, the

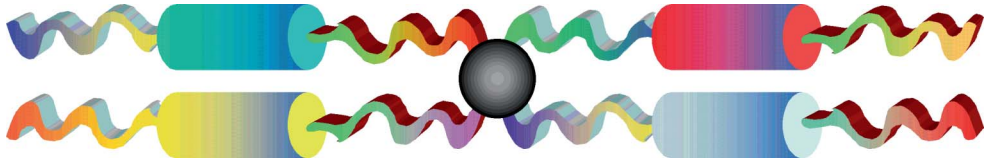

Figure 58. A multipedal tetramer showing by colour all of the variations of architectures possible. With respect to the coloured units, each has three segments which can be bound either way around giving eight variations, and for a tetramer there are two possible arrangements for the arms of the scaffold. Thus, the number of variations is 2×8^4.

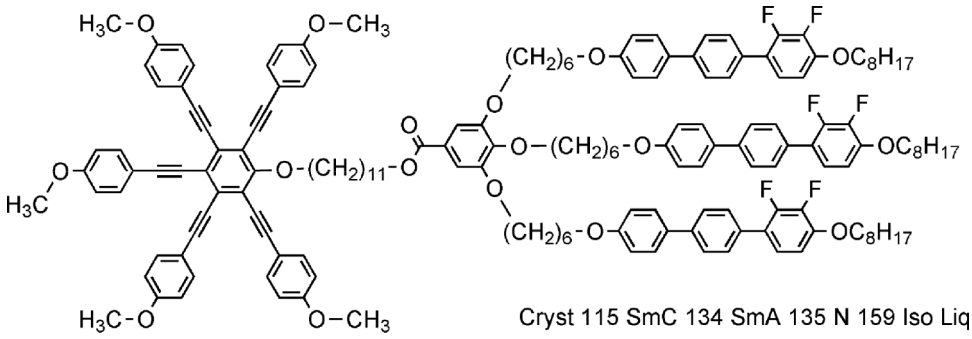

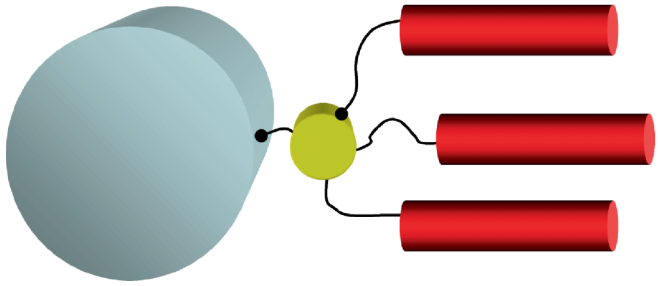

Figure 59. A supermolecular material that combines disc- and rod-like mesogens in order to give an example of a biaxial nematic phase.

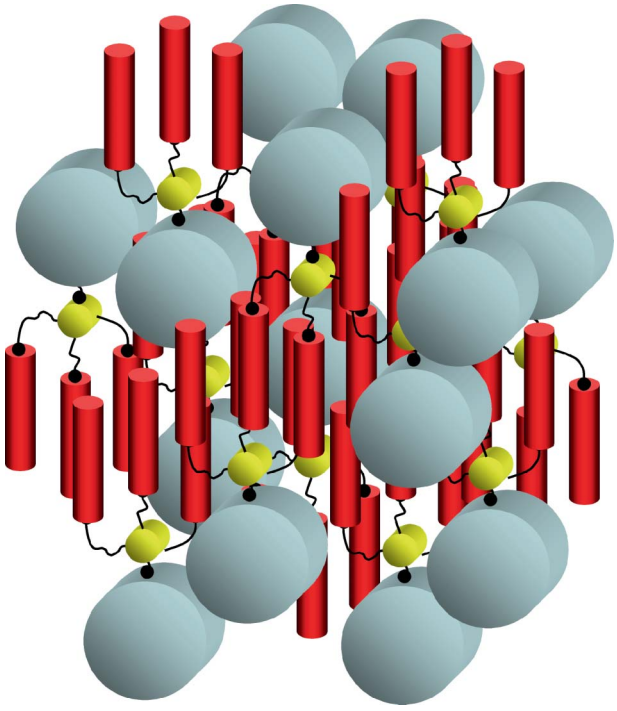

Figure 60. Local biaxial organisation in a disc-rod supermolecular material.

European Science Foundation, the University of Hull, Kingston Chemicals Ltd, Merck UK, Defence and Research Agency (DERA) and the Engineering and Physical Sciences Research Council (EPSRC) for financial support.

References

(1) Toyne, K.J. *Thermotropic Liquid Crystals*; Critical Reports on Applied Chemistry 22, Gray, G.W., Ed.; Wiley: Chichester, 1987, pp. 28–63.
(2) Demus, D.; Demus, H.; Zaschke, H. *Flüssige Kristalle in Tabellen*, VEB Deutscher Verlag für Grundstoffindustrie: Leipzig, 1974.
(3) Demus, D.; Zaschke, H. *Flüssige Kristalle in Tabellen*, Vol. II, VEB Deutscher Verlag für Grundstoffindustrie: Leipzig, 1984.
(4) Gray G.W. *Adv. Liq. Cryst*. **1976**, *2*, 39; Gray, G.W. *Advances in Liquid Crystal Materials Applications*, BDH Special Publication; BDH Chemicals Ltd: Poole, 1978.
(5) Minas, H.; Murawski, H.-R.; Stegemeyer, H.; Sucrow, W. *J. Chem . Soc., Chem. Commun.* **1982**, 308.
(6) Sucrow, W.; Minas, H.-R.; Stegemeyer, H.; Geschwinder, H.; Murawski, H.R.; Krüger, C. *Chem. Ber*. **1985**, *118*, 3322–3349.
(7) Pohl, L.; Eidenschink, R.; Krause, J.; Erdman, D. *Phys. Lett. A* **1977**, *60*, 421–423.
(8) Goodby, J.W. *The Handbook of Liquid Crystals Vol. 2A: Low Molecular Weight Liquid Crystals I*, Demus, D., Goodby, J.W., Gray, G.W., Spiess, H.-W. and Vill, V., Eds; Wiley-VCH: Weinheim, 1998, Ch. V, pp. 413–440.
(9) Gray, G.W.; Harrison, K.J.; Nash, J.A. *Electron. Lett.* **1973**, *9*, 130.
(10) Eidenschink, R.; Erdman, D.; Krause, J.; Pohl, L. *Angew. Chem., Int. Ed. Engl.* **1978**, *17*, 133–134.
(11) Osman, M.A.; Huynh-Ba, T. *Helv. Chim. Acta* **1984**, *67*, 959–963.
(12) Boller, A.; Cereghetti, M.; Schadt, M.; Scherrer, H. *Mol. Cryst. Liq. Cryst.* **1977**, *42*, 1225–1241.
(13) Carr, N.; Gray, G.W.; McDonnell, D.G. *Mol. Cryst. Liq. Cryst.* **1983**, *97*, 13–28.

(14) Lueder, E. *Liquid Crystal Displays*, 1st edn; Wiley: Chichester, 2003.
(15) Yang, D.; Wu, S. *Fundamentals of Liquid Crystal Devices*, 1st edn; Wiley: Chichester, 2006.
(16) Pauluth, D.; Tarumi, K. *J. Mater. Chem.* **2004**, *14*, 1219–1227.
(17) Kirsch, P.; Tarumi, K. *Angew. Chem. Int. Ed.* **1998**, *37*, 484–489.
(18) Klasen-Memmer, M.; Bremer, M.; Rillich, M. *US Patent 6*, *896*,*939*g *B2* (2003).
(19) Klasen, M.; Weller, C.; Tarumi, K.; Bremer, M. *US Patent 6*, *764*,*722*, *B2* (2004).
(20) Gray, G.W.; Hird, M.; Lacey, D.; Toyne, K.J. *J. Chem. Soc., Perkin Trans.* **1989**, *2*, 2041–2053.
(21) Clark, N.A.; Lagerwall, S.T. *Appl. Phys. Lett*. **1980**, *36*, 899–901.
(22) Jones, J.C.; Towler, M.J.; Hughes, J.R. *Displays* **1993**, *14*, 86–93.
(23) Perennes F.A.; Crossland W.A. *Opt. Eng.* **1997**, *36*, 2294–2301.
(24) Goodby, J.W.; Toyne, K.J.; Hird, M.; Styring, P.; Lewis, R.A.; Beer, A.; Dong, C.C.; Glendenning, M.E.; Jones, J.C.; Lymer, K.P.; Slaney, A.J.; Minter, V.; Chan L.K.M. Liquid crystal materials, devices and flat panel displays, Shashidhar, R. and Gnade, B., Eds; *Proc. SPIE*, **2000**, *3955*, 2–14.
(25) Clark, N.A.; Crandall, C.; Handschy, M.A.; Meadows, M.R.; Malzbender, R.M.; Park, C.; Xue, J.Z. *Ferroelectrics* **2000**, *246*, 1003–1016.
(26) O'Callaghan, M.J.; Ferguson, R.; Vohra, R.; Thurmes, W.; Harant, A.W.; Pecinovsky, C.S.; Zhang, Y.Q.; Yang, S.; O'Neill, M.; Handschy, M.A. *J. Soc. Inform. Display* **2009**, *17*, 369–375.
(27) Gray, G.W.; Harrison, K.J. *Mol. Cryst. Liq. Cryst.* **1971**, *13*, 37–60.
(28) Goodby, J.W.; Gray, G.W. *J. Phys. (Paris) C3* **1976**, *37*, 17–26.
(29) Chan, L.K.M.; Gray, G.W.; Lacey, D. *Mol. Cryst. Liq. Cryst.* **1985**, *123*, 185–204.
(30) Chan, L.K.M.; Gray, G.W., Lacey, D.; Toyne, K.J. *Mol. Cryst. Liq. Cryst.* **1988**, *158*, 209–240.
(31) Hird, M., PhD Thesis, The synthesis and properties of liquid crystals for twisted nematic and ferroelectric displays. University of Hull, 1990.
(32) Glendenning, M.E. PhD Thesis, Liquid crystalline materials for ferroelectric mixtures of high dielectric biaxiality. University of Hull, 1998.
(33) Glendenning, M.E.; Goodby, J.W.; Hird, M.; Toyne, K.J. *J. Chem. Soc., Perkin Trans.2*, **1999**, 481–491.
(34) Budai, J.; Pindak, R.; Davey, S.C.; Goodby, J.W *J. Phys. (Paris) Lett.* **1984**, *45*, L-1053–1062.
(35) McMillan, W.L.; *Phys. Rev. A* **1973**, *8*, 1921–1929.
(36) Wulf, A. *Phys. Rev. A* **1975**, *11*, 365–375.
(37) Priest, R.G. *J. Chem. Phys.* **1976**, *65*, 408–411.
(38) Goodby, J.W. *Mol. Cryst. Liq. Cryst.* **1981**, *75*, 179–199.
(39) Gasowska, J.S.; Cowling, S.J.; Cockett, M.C.R.; Hird, M.; Lewis, R.A.; Raynes, E.P.; Goodby, J.W., submitted.
(40) Hird, M.; Goodby, J.W.; Toyne, K.J. Liquid crystal materials, devices and flat panel displays, Shashidhar, R. and Gnade, B., Eds; *Proc. SPIE* **2000**, *3955*, 15–23.
(41) Goodby, J.W.; Gray, G.W. *Mol. Cryst. Liq. Cryst.* **1976**, *37*, 157–188.
(42) Pindak, R.; Moncton, D.E.; Davey, S.C.; Goodby, J.W. *Phys. Rev. Lett.* **1981**, *46*, 1135–1138.
(43) Pitchford, T.; Nounesis, G.; Dumrongrattana, S.; Viner, J.M.; Huang, C.C.; Goodby, J.W. *Phys. Rev. A* **1985**, *32*, 1938–1940.
(44) Goodby, J.W. *Liquid Crystals and Ordered Fluids*, Vol. 4, Johnson, J. and Griffin, A.C. Eds.; Plenum: New York, 1984, pp. 175–201.
(45) Sunohara, K.; Takatoh, K.; Sakamoto, M. *Liq. Cryst.* **1993**, *13*, 283–294.
(46) Coles, H.J.; Owen, H.; Newton, J.; Hodge, P. *Liq. Cryst.* **1993**, *15*, 739–744.
(47) Cosquer, G. PhD Thesis, Liquid crystals with novel terminal chains as ferroelectric hosts. University of Hull, 2000.
(48) Petrenko, A.; Goodby, J.W. *J. Mater. Chem*. **2007**, *17*, 766–782.
(49) Inui, S.; Iimura, N.; Suzuki, T.; Iwane, H.; Miyachi, K.; Takanishi, Y.; Fukuda, A. *J. Mater. Chem.* **1996**, *6*, 671–673.
(50) Nishiyama, I.; Goodby, J.W. *J. Mater. Chem.* **1992**, *2*, 1015–1023.
(51) 51. Gasowska, J.S.; Cowling, S.J.; Hird, M.; Lewis, R.A.; Goodby, J.W., submitted.
(52) Nishiyama, I.; Goodby, J.W. *J. Mater. Chem.* **1993**, *3*, 149–159.
(53) Goodby, J.W. *Mol. Cryst. Liq. Cryst.* **1997**, *292*, 245–263.
(54) Yoshizawa, A.; Nishiyama, I.; Kikuzaki, H.; Ise, N. *Jpn. J. Appl. Phys.* **1992**, *31*, L860–L863.
(55) Yoshizawa, A.; Yokoyama, N.A.; Kikuzaki, H.; Hirai, T. *Liq. Cryst.* **1993**, *14*, 513–523.
(56) Yoshizawa, A.; Kikuzaki, H.; Fukumasa, M. *Liq. Cryst.* **1995**, *18*, 351–366.
(57) Bartolino, R.; Doucet, J.; Durand, G. *Ann. Phys.* **1978**, *3*, 389–395.
(58) Miyachi, K.; Fukuda, A. *Handbook of Liquid Crystals Vol. 2B: Low Molecular Weight Liquid Crystals II*, Demus, D., Goodby, J.W., Gray, G.W., Spiess H.-W. and Vill, V., Eds; Wiley-VCH, Weinheim, 1998, pp. 665–691.
(59) Lee, S.-E. PhD Thesis, Antiferroelectric and ferroelectric liquid crystals in terphenyl systems. University of Hull, 1998.
(60) Goodby, J.W.; Saez, I.M.; Cowling, S.J.; Görtz, V.; Draper, M.; Hall, A.W.; Sia, S.; Cosquer, G.; Lee, S.-E.; Raynes, E.P. *Angew. Chem. Int. Ed.* **2008**, *47*, 2754–2787.
(61) Chandani, A.D.L.; Gorecka, E.; Ouchi, Y.; Takezoe, H.; Fukuda, A. *Jpn. J. Appl. Phys.* **1989**, *29*, L1265–L1268.
(62) Inui, S.; Suzuki, T.; Iimura, N.; Iwane, H.; Nohira, H. *Ferroelectrics* **1994**, *148*, 79–84.
(63) Goodby, J.W. *J. Mater. Chem*. **1991**, *1*, 307–318.
(64) Goodby, J.W.; Cowling, S.J.; Görtz, V. *Comptes Rend. Chimie* **2009**, *12*, 70–84.
(65) Goodby, J.W.; Chin, E.; Leslie, T.M.; Geary, J.M.; Patel, J.S. *J. Am. Chem. Soc.* **1986**, *108*, 4729–4735.
(66) Cowling S.J.; Goodby, J.W. *Chem. Commun.* **2006**, *39*, 4107–4109.
(67) Patel, J.S.; Goodby, J.W. *Phil. Mag. Lett.* **1987**, *55*, 283–287.
(68) Goodby, J.W.; Chin, E.; Geary, J.M.; Patel, J.S.; Finn, P.L. *J. Chem. Soc. Faraday Trans. 1* **1987**, *83*, 3429–3446.
(69) Watson, M.J.; Horsburgh, M.K.; Goodby, J.W.; Takatoh, K.; Slaney, A.J.; Patel, J.S.; Styring, P. *J. Mater. Chem.* **1998**, *8*, 1963–1969.
(70) Ornstein, L.S.; Kast, W. *Trans. Faraday Soc*. **1933**, *29*, 931–944.

(71) Glass, A.M.; Patel, J.S.; Goodby, J.W.; Olson, D.H.; Geary, J.M. *J. Appl. Phys.* **1986**, *60*, 2778–2782.
(72) Neal, M.P.; Solymosi, M.; Wilson, M.R.; Earl, D.J. *J. Chem. Phys.* **2003**, *119*, 3567–3573.
(73) Kamberaj, H.; Osipov, M.A.; Low, R.J.; Neal, M.P. *Mol. Phys.* **2004**, *102*, 431–446.
(74) Kamberaj, H.; Low, R.J.; Neal, M.P. *Ferroelectrics* **2005**, *315*, 183–196.
(75) Kamberaj, H.; Low, R.J.; Neal, M.P. *Mol. Phys.* **2006**, *104*, 335–357.
(76) Cowling, S.J.; Toyne, K.J.; Goodby, J.W. *Mol. Cryst. Liq. Cryst*. **1999**, *332*, 2981–2994.
(77) Cowling, S.J.; Toyne, K.J.; Goodby, J.W. *J. Mater. Chem*. **2001**, *11*, 1590–1599.
(78) Watson, P. PhD Thesis, The use of diallylamine in photocurable liquid crystal systems. University of York, 2007.
(79) Goodby, J.W.; Toyne, K.J.; Hird, M.; Styring, P.; Lewis, R.A.; Beer, A.; Dong, C.C.; Glendenning, M.E.; Jones, J.C.; Lymer, K.P.; Slaney, A.J.; Minter, V.; Chan, L.K.M. *Mol. Cryst. Liq. Cryst.* **2000**, *346*, 169–182.
(80) Imrie, C.T.; Henderson, P.A. *Chem. Soc. Rev*. **2007**, *36*, 2096–2128.
(81) Imrie, C.T.; Henderson, P.A. *Curr. Opin. Colloid Interface Sci*. **2002**, *7*, 298–311.
(82) Sia, S. PhD Thesis, Molecular crowding and microphase segregation in supermolecular liquid crystals. University of Hull, 2004.
(83) Hardouin, F.; Achard, M.F.; Jin, J.-I.; Shin, J.-W.; Yun, Y.-K. *J. Phys. II (Paris)* **1994**, *4*, 627–643.
(84) Imrie, C.T.; Luckhurst, G.R. *J. Mater. Chem.* **1998**, *8*, 1339–1343.
(85) Griffin, A.C.; Sullivan, S.L.; Hughes, W.E. *Liq. Cryst.* **1989**, *4*, 677–684.
(86) Nishiyama, I.; Yamamoto, J.; Goodby, J.W.; Yokoyama, H. *J. Mater. Chem.* **2001**, *11*, 2690–2693.
(87) Nishiyama, I.; Yamamoto, J.; Goodby, J.W.; Yokoyama, H. *J. Mater. Chem.* **2002**, *12*, 1709–1716.
(88) Nishiyama, I.; Yamamoto, J.; Goodby, J.W.; Yokoyama, H. *Liq. Cryst.* **2002**, *29*, 1409–1423.
(89) Nishiyama, I.; Yamamoto, J.; Goodby, J.W.; Yokoyama, H. *Ferroelectrics* **2002**, *276*, 255–265.
(90) Nishiyama, I.; Yamamoto, J.; Goodby, J.W.; Yokoyama, H. *J. Mater. Chem.* **2003**, *13*, 1868–1876.
(91) Nishiyama, I.; Yamamoto, J.; Goodby, J.W.; Yokoyama, H. *J. Mater. Chem.* **2003**, *13*, 2429–2435.
(92) Nishiyama, I.; Yamamoto, J.; Yokoyama, H.; Goodby, J.W. *Mol. Cryst. Liq. Cryst.* **2003**, *400*, 21–29.
(93) Nishiyama, I.; Yamamoto, J.; Yokoyama, H.; Mery, S.; Guillon, D.; Goodby, J.W. *Trans. Mats. Res. Soc. Jpn.* **2004**, *29*, 785–788.
(94) Nishiyama, I.; Yamamoto, J.; Goodby, J.W.; Yokoyama, H. *Chem. Mats.* **2004**, *16*, 3212–3214.
(95) Nishiyama, I.; Yamamoto, J.; Goodby, J.W.; Yokoyama, H. *Liq. Cryst.* **2004**, *31*, 1495–1502.
(96) Nishiyama, I.; Yamamoto, J.; Goodby, J.W.; Yokoyama, H. *Proc. SPIE* **2004**, *5518*, 201–210.
(97) Nishiyama, I.; Yamamoto, T.; Yamamoto, J.; Yokoyama, H.; Goodby, J.W. *Mol. Cryst. Liq. Cryst.* **2005**, *439*, 1921–1931.
(98) Goodby, J.W.; Pindak, R. *Mol. Cryst. Liq. Cryst.* **1981**, *75*, 233–247.
(99) Goodby, J.W. *Mol. Cryst. Liq. Cryst. Lett.* **1981**, *72*, 95–99.
(100) Percec, V.; Mitchell, C.M.; Cho, W.-D.; Uchida, S.; Glodde, M.; Ungar, G.; Zeng, X.; Liu, Y.; Balagurusamy, V.S.K.; Heiney, P.A. *J. Am. Chem. Soc*. **2004**, *126*, 6078–6094.
(101) Percec, V.; Peterca, M.; Sienkowska, M.J.; Ilies, M.A.; Aqad, E.; Smidrkal, J.; Heiney, P.A. *J. Am. Chem. Soc*. **2006**, *128*, 3324–3334.
(102) Percec, V.; Cho, W.-D.; Ungar, G.; Yeardley, D.J.P. *J. Am. Chem. Soc.* **2001**, *123*, 1302–1315.
(103) Percec, V.; Dulcey, A.E.; Balagurusamy, V.S.K.; Miura, Y.; Smidrkal, J.; Peterca, M.; Nummelin, S.; Edlund, U.; Hudson, S.D.; Heiney, P.A.; Hu, D.A.; Magonov, S.N.; Vinogradov, S.A. *Nature* **2004**, *430*, 764–768.
(104) Percec, V. *Philos. Trans. R. Soc.* **2006**, *364*, 2709.
(105) Saez, I.M.; Goodby, J.W.; Richardson, R.M. *Chem. Euro. J.* **2001**, *7*, 2758–2764.
(106) Campidelli, S.; Brandmüller, T.; Hirsch, A.; Saez, I.M.; Goodby, J.W.; Deschenaux, R. *Chem. Comm.* **2006**, 4282–4284.
(107) Nelson, D.R. *Nanolett.* **2002**, *2*, 1125–1129.
(108) Fernandez-Nieves, A.; Vitelli, V.; Utada, A.S.; Link, D.R.; Marquez, M.; Nelson, D.R.; Weitz, D.A. *Phys. Rev. Lett.* **2007**, *99*, 157801.
(109) Vitelli, V.; Nelson, D.R. *Phys. Rev. E* **2006**, *74*, 021711.
(110) Bates, M.A. *J. Chem. Phys.* **2008**, *128*, 104707.
(111) Bates, M.A. *Soft Matter* **2008**, *4*, 2059–2063.
(112) Saez, I.M.; Goodby, J.W. *J. Mater. Chem*. **2003**, *13*, 2727–2739.
(113) Zab, K.; Joachimi, D.; Agert, O.; Neumann, B.; Tschierske, C. *Liq. Cryst*. **1995**, *18*, 489–494.
(114) Saez, I.M.; Goodby, J.W. *Chem. Commun.* **2003**, 1726–1727.
(115) Saez, I.M.; Goodby, J.W. *Chem. Eur. J.* **2003**, *9*, 4869–4877.
(116) Kouwer, P.H.J.; Mehl, G.H. *Mol. Cryst. Liq. Cryst.* **2003**, *397*, 301–316.
(117) Kouwer, P.H.J.; Mehl, G.H.; Picken, S.J. *Mol. Cryst. Liq. Cryst.* **2004**, *411*, 1429–1438.
(118) Kouwer, P.H.J.; Mehl, G.H. *Angew. Chem. Int. Ed. Engl*. **2003**, *42*, 6015–6018.